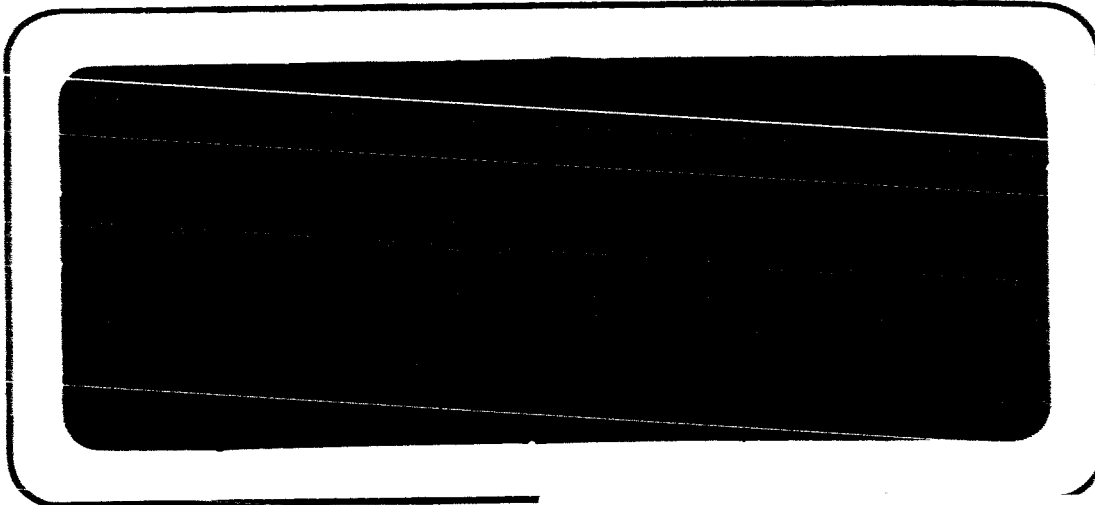


1100001365486



N66 35661

(ACCESSION NUMBER)

29

(PAGES)

OK-15486

(IN ALA OR OR TMX OR AD NUMBER)

(TITLE)

1

(CODE)

33

(CATEGORY)

TRW SYSTEMS

ONE SPACE PARK • REDONDO BEACH, CALIFORNIA

GPO PRICE \$ _____

OFFER PRICE(S) \$ _____

Hard copy (HC) \$ 1.00

Microfiche (MF) \$ 1.75

MAR 80 JUN 80

DETERMINATION OF THERMOPHYSICAL PROPERTIES
OF ABLATIVE MATERIALS

PHASE I - LABORATORY DETERMINATIONS

LIBRARY COPY

AUG 29 1966

MANNED SPACECRAFT CENTER
HOUSTON, TEXAS

Part A - Heat Capacity, Density, Decomposition
and Melt Temperature

Stumenthal, R. D. Larson, R. C. Nordberg

July 1, 1966

Contract NAS9-4518

Approved:

E. A. Burns
E. A. Burns,
Phase I Manager

F. E. Arndt
F. E. Arndt,
Program Manager

B. Dubrow
B. Dubrow, Manager
Chemistry Department

Technical Management
NASA Manned Spacecraft Center
Houston, Texas
D. G. Stafford
Primary Propulsion Branch

TRW Systems
One Space Park
Redondo Beach, California

ACKNOWLEDGEMENT

The authors express their appreciation to the many individuals who have contributed to this study. In particular the efforts of J. Kliegel, Manager, Propulsion Analysis Department, who provided overall program supervision, Fred E. Arndt, Program Manager, B. Dubrow, Head, Chemistry Department, who provided Phase I program supervision and E. A. Burns, Head, Applied Chemistry Section who performed as Phase I manager. The many significant contributions of Members of the Technical Staff, D. F. Carrol and Technical Support personnel M. J. Santy, and G. F. Charlan are gratefully acknowledged.

ABSTRACT

This report describes the work performed under Contract NAS9-4518 to perform laboratory measurements of thermophysical properties of three ablative materials being used on the Apollo Spacecraft primary propulsion systems. Two additional materials were also evaluated which have potential as improved ablative materials for Apollo applications. The thermophysical properties reported here are comprised of heat capacity, density, decomposition temperature and melt temperature. The thermophysical properties were determined on Fiberite Corporation MX 2600 and MX 2646, Western Backing Corporation WBC 2234 and WBC 5217, and U. S. Polymeric Corporation XR 2015. Descriptions of the experimental techniques and interpretation and discussions of the test results are presented for each of the thermophysical properties.

SUMMARY

This report describes the work performed by TRW Systems for the National Aeronautics and Space Administration, Manned Spacecraft Center, on Phase IA under Contract NAS9-4518. The primary objective of Phase I of this program was to perform laboratory measurements for the determination of thermophysical properties of selected virgin and charred ablative materials as a function of temperature. The thermophysical properties determined in Phase IA, and reported here, comprise heat capacity, density, decomposition temperature and melt temperature.

Heat capacity measurements were conducted as a function of temperature on both virgin and charred materials. Measurements on the virgin materials were made utilizing a Perkin-Elmer Model DSC-1 Differential Scan Calorimeter. The heat capacity of the charred materials was measured in the temperature range of 630 °F to 1710 °F with a modified Smith Calorimeter. There was good agreement between measurements made with the Differential Scan Calorimeter and the Smith Calorimeter. In general, the Smith Calorimeter data were slightly higher. An extrapolation of these data to 3000 °F is provided.

Bulk density measurements in the temperature range of 77 °F to 1652 °F were conducted with 3/4-inch cube samples of each of the five virgin and charred ablative materials. Densities were computed based on the weight of the sample after exposure for one hour and on the steady state volume of the sample at the experimental temperature.

Thermogravimetric traces (TGA curves) were obtained using an Aminco Thermo-Grav to determine the resin decomposition temperature for all materials. The general shape of all the TGA curves were similar. It was determined that a specific decomposition temperature cannot be defined, but rather that decomposition occurs over a narrow temperature range. Rapid resin decomposition is observed to begin at about 600 °F with complete resin decomposition occurring at about 1000 °F.

The temperature at which charred specimens of each of the five ablative materials either formed a liquid phase or rapidly decomposed was measured in a tungsten ribbon melting point furnace. In addition, for the four materials which formed carbon-silica chars (MX2600, MX2646, WBC2234 and XR2015), measurements were made of the rate of carbon monoxide formation due to the reaction of carbon with silica.

CONTENTS

	Page
ACKNOWLEDGEMENT	ii
ABSTRACT	iii
SUMMARY	iv
1.0 INTRODUCTION	1
2.0 MATERIALS INVESTIGATED	3
3.0 HEAT CAPACITY MEASUREMENTS	5
3.1 Experimental Techniques	5
3.1.1 Heat Capacity Measurements Using the Differential Scan Calorimeter	5
3.1.2 Heat Capacity Measurements Using a Modified Smith Calorimeter	8
3.1.3 Preparation of Charred Specimens	16
3.2 Experimental Results	17
3.2.1 Heat Capacity Measurements on Virgin Ablative Materials	17
3.2.2 Heat Capacity Measurements on Charred Ablative Materials	17
3.3 Recommended Heat Capacity Data	26
4.0 BULK DENSITY MEASUREMENTS	30
4.1 Experimental Procedure	30
4.2 Experimental Results	31
5.0 RESIN DECOMPOSITION TEMPERATURE	43
5.1 Operation of the Thermobalance	43
5.2 Experimental Results	45
6.0 MEASUREMENT OF CHAR MELTING AND DECOMPOSITION TEMPERATURES	52
6.1 Char Melting Experiments	52
6.2 Temperature Scan Experiments	57

TABLES

2.1	Ablative Materials Investigated	4
2.2	Weight Loss on Ignition of Ablative Materials	4
3.1	Temperature Time Profile for Charring the MX 2646 Specimen . .	18
3.2	Weight Loss on Charring Specimens for Heat Capacity Measurements	19
3.3	Summary of Heat Capacity Measurements on Virgin Ablative Materials	22
3.4	Heat Capacity Measurements on the Charred Ablative Materials	25
3.5	Recommended Heat Capacities in Virgin Materials	26
3.6	Recommended Heat Capacities of Charred Materials	27
4.1	Density Measurement Data for MX 2600	32
4.2	Density Measurement Data for MX 2646	33
4.3	Density Measurement Data for XR 2015	34
4.4	Density Measurement Data for WBC 2234	35
4.5	Density Measurement Data for WBC 5217	36
5.1	Summary of Weight Loss Measurements for Thermogravi- metric Analyses of Ablative Materials	51
6.1	Charred MX 2600 Melting Experiment	53
6.2	Charred XR 2015 Melting Experiment	55
6.3	Charred MX 2646 Melting Experiment	55
6.4	Charred WBC 2234 Melting Experiment	56
6.5	Charred WBC 5217 Melting Experiment	56

ILLUSTRATIONS

	Page
3.1 Perkin-Elmer DSC -1 Differential Scan Calorimeter	6
3.2 Typical Differential Calorimetric Heat Capacity Scans	7
3.3 Arrangement of Charred Specimens in the Smith Heat Capacity Measurement Method	10
3.4 Photograph of Smith Calorimeter Showing Inner and Outer Nickel Containers.	11
3.5 Photograph of Assembled Calorimeter Ready to Place in the Furnace.	12
3.6 Astro Furnace and Calorimeter Assembly	14
3.7 Graphite Heat Capacity	15
3.8 Charred Ablative Specimens for Smith Calorimetry	20
3.9 WBC 5217 Charred Ablative Specimen for Smith Calorimetry . .	21
3.10 Heat Capacity as a Function of Temperature for Virgin Samples of XR 2015, MX 2646, and MX 2600	23
3.11 Heat Capacity as a Function of Temperature for Virgin Samples of WBC 5217 and WBC 2234	24
3.12 Heat Capacity vs. Temperature Data for the Five Charred Ablative Materials	29
4.1 Steady State Bulk Density vs. Temperature Measurements for the Five Ablative Materials	37
4.2 Photograph of MX 2600 Before and After Heating to 1652°F . . .	38
4.3 Photograph of MX 2646 Before and After Heating to 1652°F . . .	39
4.4 Photograph of WBC 5217 Before and After Heating of 1652°F . .	40
4.5 Photograph of XR 2015 Before and After Heating of 1652°F . . .	41
4.6 Photograph of WBC 2234 Before and After Heating of 1652°F . .	42
5.1 Aminco Thermograv.	44

ILLUSTRATIONS (continued)

	Page
5.2 Thermogram of MX 2600	46
5.3 Thermogram of MX 2646	47
5.4 Thermogram of WBC 5217	48
5.5 Thermogram of XR 2015	49
5.6 Thermogram of WBC 2234	50
6.1 High Temperature Reaction Kinetics System	58
6.2 Thermal Decomposition of MX 2600 Char	59
6.3 Thermal Decomposition of MX 2646 Char	60
6.4 Thermal Decomposition of XR 2015 Char	61
6.5 Thermal Decomposition of WBC 2234 Char	62

1.0 INTRODUCTION

This report describes a portion of the work performed on the Study to Determine Thermophysical Properties of Ablative Materials for the National Aeronautics and Space Administration, Manned Spacecraft Center, under Contract NAS9-4518. The primary objective of this program is to determine the thermophysical properties of selected ablative materials being used or contemplated for use on the Apollo Spacecraft liquid rocket engines. This report describes the work conducted in Phase IA of the Phase I effort for determining the thermophysical properties of ablative materials. Under Phase I laboratory measurements were performed to determine the following thermophysical properties, as a function of temperature for each of the five materials investigated:

- Heat capacity (both char and virgin)
- Density (both char and virgin)
- Decomposition temperature
- Melt temperature
- Thermal conductivity (both char and virgin)
- Thermal diffusivity (both char and virgin).

These property variations were determined as a function of temperature up to 1800 °F. The data were extrapolated from 1800 °F to 3000 °F. All property data, with the exception of the thermal conductivity data, are presented in this Phase IA report. The Phase IB report will cover the thermal conductivity measurements and the results of the thermal diffusivity calculations. Under Phase II of the program, well instrumented engine firings will be conducted with a 1000-lb thrust rocket engine utilizing ablative thrust chambers made from the identical materials investigated in Phase I.

The comparative results from laboratory measurements and engine measurements are expected to determine whether thermophysical property data obtained from controlled laboratory measurements can be adequately extrapolated analytically to that observed in a dynamic engine firing. Furthermore, these data significantly improve the capability of analytical predictions of ablative material behavior in rocket engine environments.

This report is divided into five principal sections. The first section describes the five ablative materials that were investigated. The next four sections cover the following thermophysical property measurements:

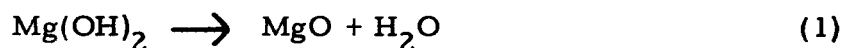
- Heat capacity (both char and virgin)
- Density (both char and virgin)
- Decomposition temperature
- Melt temperature.

In each of these sections a detailed discussion is provided of the techniques employed, together with the results obtained for the five ablative materials.

2.0 MATERIALS INVESTIGATED

The thermophysical property measurements were conducted on the five ablative materials identified in Table 2.1. Characterization of these materials consisted of determining the resin content of the composite material. Standard analytical procedures were employed in which weighed specimens were ignited in air at 1800 °F for 16 hours, followed by cooling and determination of the weight loss. The results of these tests are listed in Table 2.2.

The weight loss figures reported in Table 2.2 approximate the resin content of all materials with the exception of WBC 5217. The weight loss for the material includes a substantial contribution from the water evolved from the hydrated magnesium hydroxide fibers. Although no measurements were conducted to determine the percentage of water in the magnesium hydroxide $\text{[Mg(OH)}_2\text{]}$ fibers in WBC 5217, the elemental balance shows that pure Mg(OH)_2 fibers undergoing decomposition yield approximately 32% w/w of water vapor, in accordance to Equation 1.



It has been reported¹ that 30.5% of this water is released below 1400 °F with 22% released between approximately 600 °F and 900 °F. The thermograms of WBC 5217 presented in Section 5.0 appear to support this information.

¹ Johns-Manville, Aerospace Bulletin No. 12, dated 15 November 1963.

TABLE 2.1
ABLATIVE MATERIALS INVESTIGATED

DESIGNATION	SUPPLIER	DESCRIPTION
MX 2600	Fiberite Corporation	Silica fabric and phenolic resin with a silica filler.
MX 2646	Fiberite Corporation	Silica fabric with a polyamide modified phenolic resin-no filler.
WBC 2234	Western Backing Corporation	"Irish Refrasil" with "high char" resin system.
WBC 5217	Western Backing Corporation	Magnesium hydroxide bulk fibers impregnated with a "high char" resin.
XR 2015	U.S. Polymeric Corporation	Silica fabric with elastomer modified, silica filled resin.

TABLE 2.2
WEIGHT LOSS ON IGNITION OF ABLATIVE MATERIALS

ABLATIVE MATERIAL	WEIGHT LOSS, % w/w
MX 2600	34.4
MX 2646	23.4
WBC 2234	34.2
WBC 5217	47.8
XR 2015	39.1

3.0 HEAT CAPACITY MEASUREMENTS

The heat capacity of samples of the five virgin ablative materials and charred specimens of each of the materials was determined as a function of temperature. The experimental techniques employed and the results obtained are presented in the following paragraphs.

3.1 EXPERIMENTAL TECHNIQUES

3.1.1 Heat Capacity Measurements Using the Differential Scan Calorimeter

Heat capacity measurements of virgin ablative materials and low temperature heat capacity measurements of charred ablative materials were made using a Perkin-Elmer Model DSC-1 Differential Scan Calorimeter. This instrument (illustrated in Figure 3.1) provides a rapid and convenient method for determination of the thermal energy involved in taking a sample through a temperature excursion. The operation of the calorimeter was as follows:

A sample was placed in one side of a two-container holder. The other side of the holder was utilized as a reference cell. As the sample goes through a change in temperature, such that an endothermic or an exothermic change occurs, energy equivalent to the thermal change is applied to maintain the sample and reference cell at the same temperature. By appropriate electronic feedback networks, the energy required (output of the wattmeter) is seen as a displacement on a recording potentiometer. For the heat capacity measurements, a sapphire reference standard was used.

The operation and calculation of heat capacities using this method are presented in the following example for MX 2600 at 286°F. The differential calorimetric scans for the sample pan blank, sample plus pan and sapphire reference plus pan are presented in Figure 3.2 for the temperature scan of 260 to 298°F at a scanning rate of 18°F/minute. It is seen that the pen rose rapidly to a new value and equilibrated after about a minute. The scanning

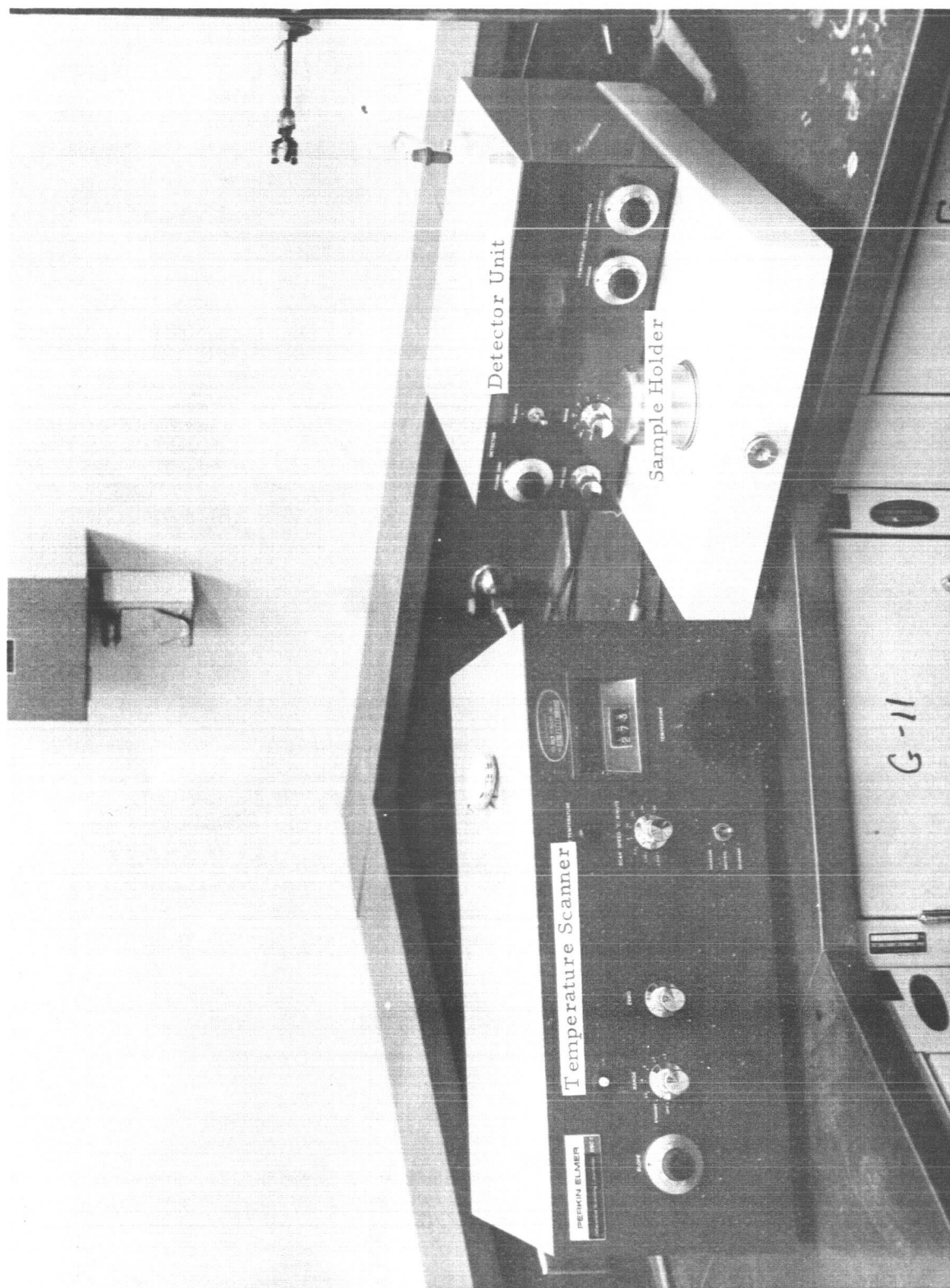


Figure 3.1 Perkin-Elmer DSC-1 Differential Scan Calorimeter

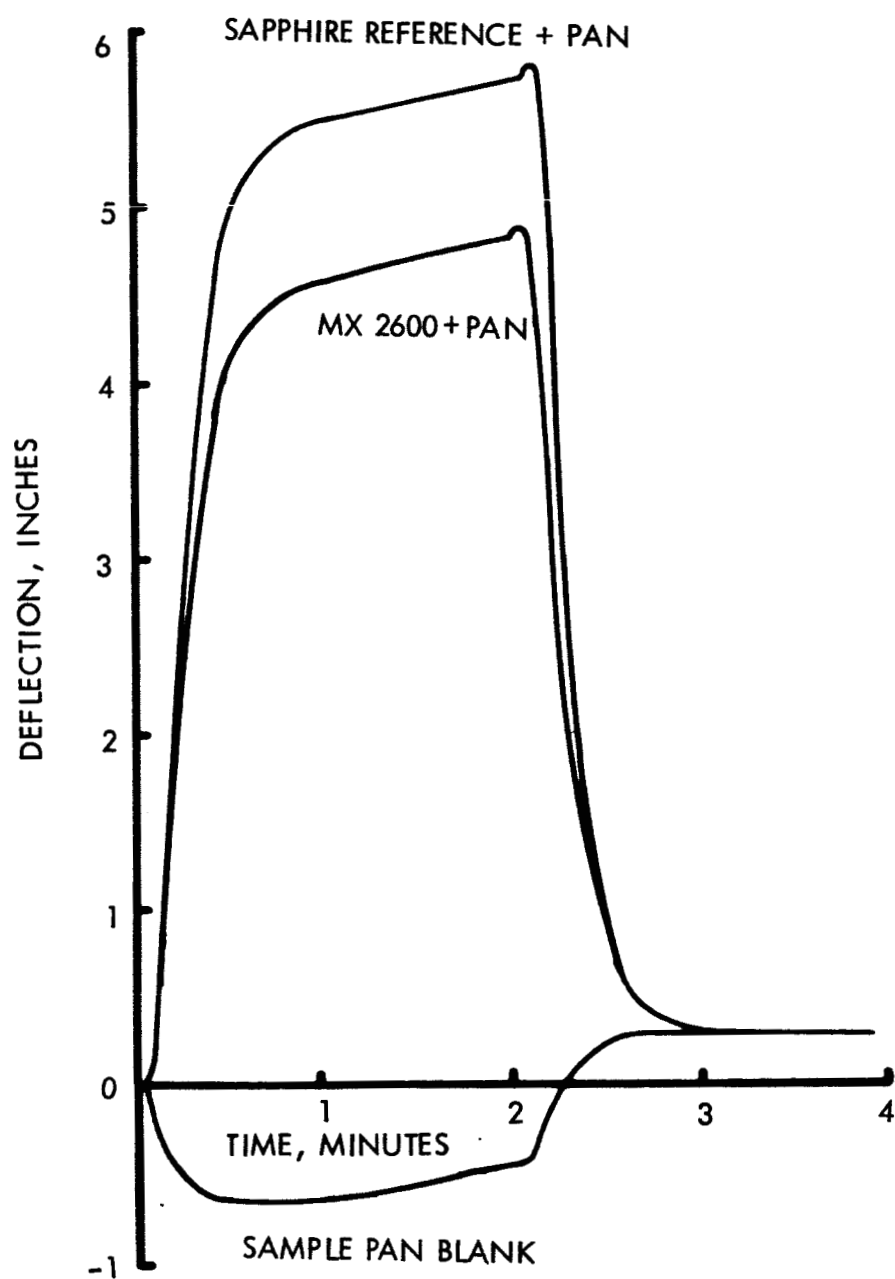


Figure 3.2 Typical Differential Calorimetric Scans
Sapphire 125.4 mg, MX 2600 86.9 mg.

was continued for about another minute and the recorder was allowed to operate after terminating the scan. The recorder pen returned to approximately the same level prior to heating the specimen to 298°F. Base lines were interpolated between the starting and final base line sections and the differences in heights between the curves and the base line were measured at 286°F (mid point equilibrated section of the curve).

The heat capacity C_x , of the sample was calculated as follows:

$$C_x = \left(\frac{L_x - L_o}{L_r - L_o} \right) \left(\frac{W_r}{W_x} \right) C_r \quad (1)$$

Where L_x = deflection of sample plus pan from base line, inches
 L_r = deflection of sapphire reference plus pan from base inches
 L_o = deflection of sample pan from base line, inches
 W_r = weight of sapphire reference, mg
 W_x = weight of sample, mg
 C_r = heat capacity of sapphire, BTU/lb°F.

Experiments were conducted on each virgin material over the temperature range from 126°F to 441°F and on each charred specimen over the temperature range from 126°F to 864°F. The reproducibility of this method was generally better than 5% relative.

3.1.2 Heat Capacity Measurements Using a Modified Smith Calorimeter

Measurements of the heat capacity of charred specimens of the ablative materials in the temperature range from 630°F to 1710°F were conducted with a modified Smith Calorimeter. Experimentally, the set-up consisted of a specimen mounted in a low thermal conductivity container with thermocouples located within the specimen and a differential thermocouple located on either side of the container walls. The container assembly was then heated at a rate governed by the differential thermocouple which was

pre-set to maintain a constant temperature difference across the container wall. Because the thermal conductivity of the container was nearly constant, the heat flow through it was nearly constant. Consequently, the heat flux to the specimen in a given elapsed time was essentially constant. Actually, the conductivity of any refractory container does not remain exactly constant as the temperature changes, and hence, the heat flow varies slightly with temperature. However, by appropriate calibration over a range of temperatures with a sample of known specific heat, reproducible quantitative results were obtained with a given container.

Figure 3.3 shows a schematic diagram of the specimen, container and thermocouple set-up. The charred specimens in the form of cylinders approximately 0.75-inch in diameter and 1.50-inch long were contained in a thin walled nickel container which was mounted inside a second larger thin walled nickel container. The space between the inner and outer nickel containers was filled with Dyna-Quartz high temperature silica insulation. Figure 3.4 shows a photograph of the calorimeter with the top removed, and Figure 3.5 shows a photograph of the assembled calorimeter ready to be placed in the furnace.

The charred specimen was instrumented with chromel-alumel thermocouples placed within the sample at several locations in order to measure precisely point sample temperatures, temperature gradients (if any, within the sample) and to obtain a value for the average sample temperature. Temperature measurement was made with a Minneapolis-Honeywell Model 2732 precision potentiometer. As shown in the schematic diagram, a differential thermocouple with one junction on the outside wall of the container and one junction on the inside wall was utilized to measure and control the temperature gradient across the container wall. The output of this thermocouple was fed to a Barber-Coleman MMC temperature control system which controlled the furnace heat input to maintain the temperature gradient across the container at a constant, pre-set value while the sample and its container were slowly heated.

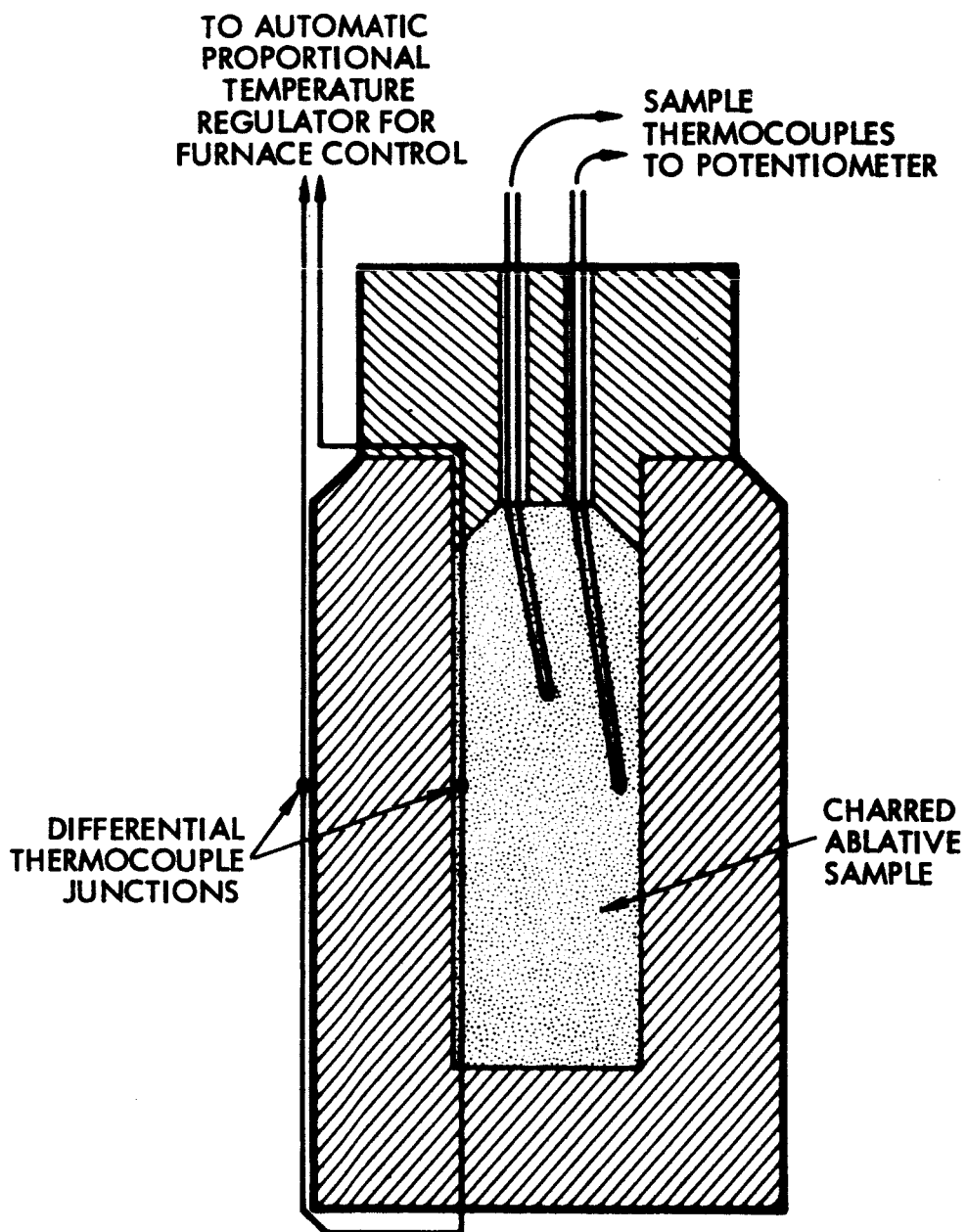


Figure 3.3 Arrangement of Charred Specimens in the Smith Heat Capacity Measurement Method



Figure 3.4 Photograph of Smith Calorimeter Showing Inner and Outer Nickel Containers

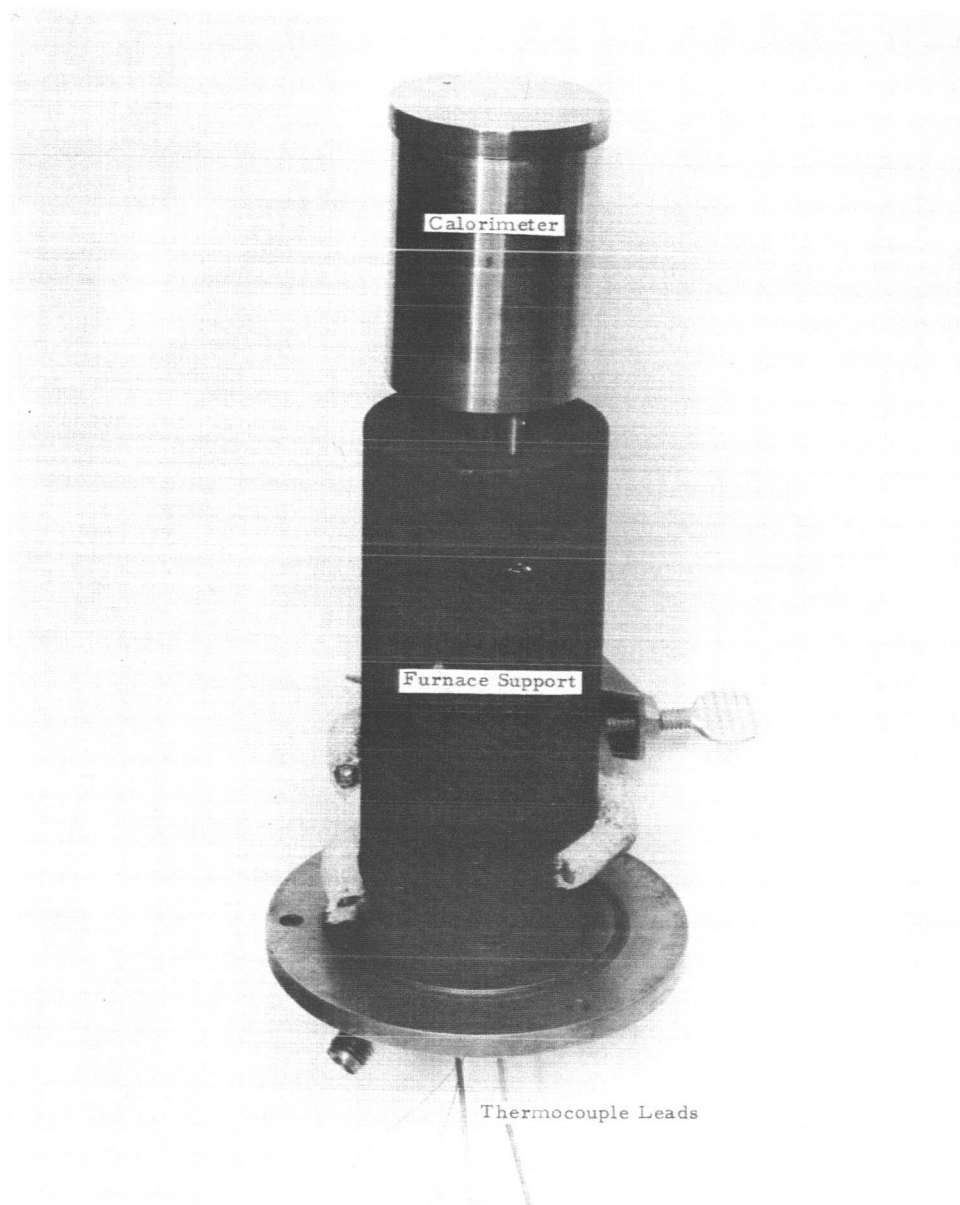


Figure 3.5 Photograph of Assembled Calorimeter Ready to Place in the Furnace

The sample-container-thermocouple assembly was heated in an Astro Model No. 2570 carbon element furnace which has a temperature capability of 3000°C. The furnace was operated in an inert argon atmosphere which protected both the heating element and the carbon-silica char sample from oxidation. Figure 3.6 shows a photograph of the Astro Furnace with the calorimeter assembly ready to be placed in the furnace.

In order to make quantitative heat measurements, it was necessary first to calibrate the container by determining its rate of heating when empty and then with a sample of known specific heat. Pure graphite was used as the primary standard since it underwent no transformations in the temperature range of interest and its heat capacity was well established from the literature. The heat capacity of a sample of the graphite standard material was checked with the differential scan calorimeter using ultra high purity copper as the standard. Figure 3.7 compares the DSC measurements with the data reported in the literature for pure graphite. It is apparent from this graph that the DSC measured heat capacities for the graphite sample were quite close to the values reported in the literature.

The rate of heat flow through the container was equal to the product of its conductivity and a geometric constant, multiplied by the temperature difference between its inner and outer surfaces. With a given container the first two factors were identical and the temperature difference was maintained constant experimentally. The resulting constant heat flow served to supply the specific heat of the sample, its heat of transformation, if any, and the specific heat of an indeterminate part of the container itself, i.e.,

$$H \times \Delta t_1 = \Delta T_1 \times C_r W_r + L_1 W_1 + \Delta T_1 \times C_l W_l, \quad (2)$$

where H is the heat flow per unit time, C_r , C_l and W_r , W_l are the specific heats and masses of the effective part of the container and of the specimen, respectively; ΔT is the change of temperature in time, t; and L_1 is the

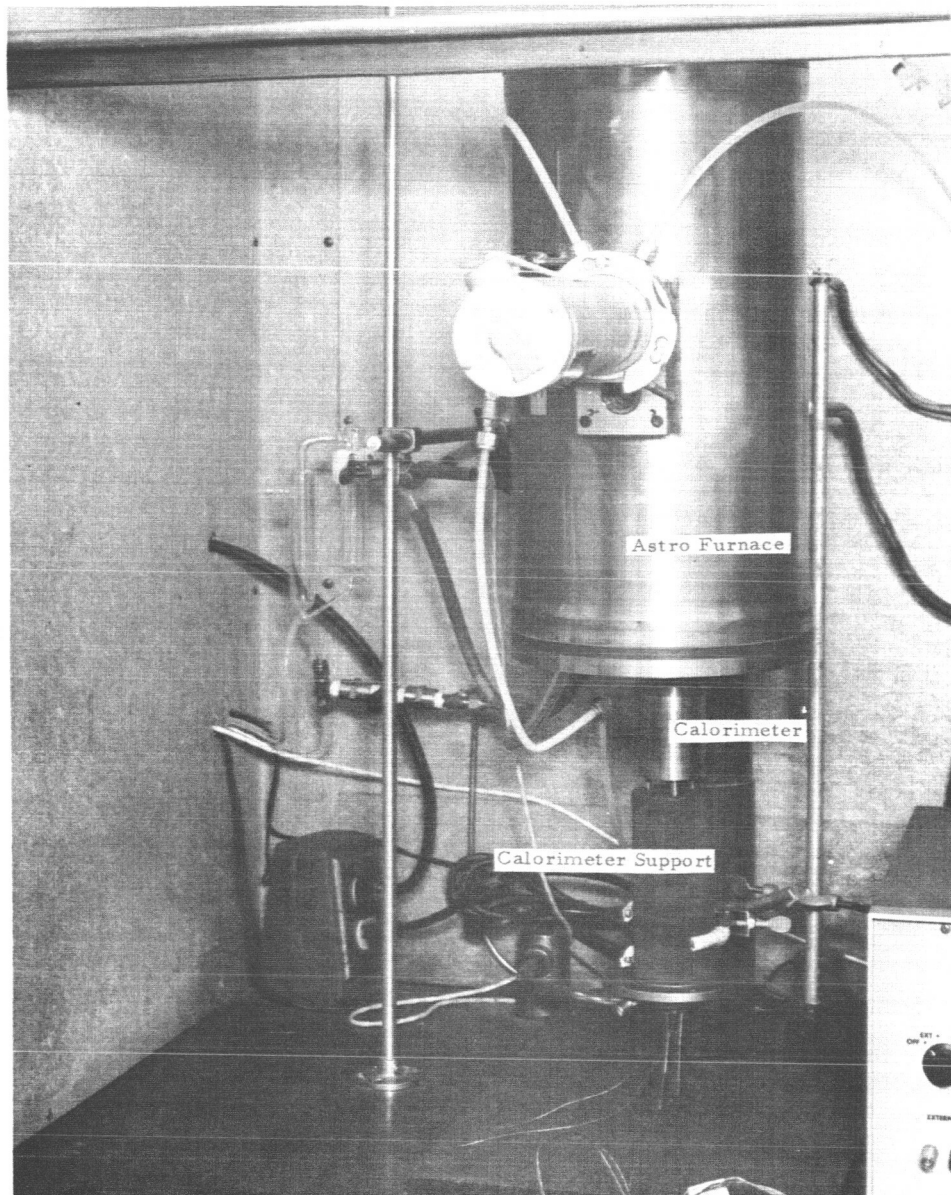
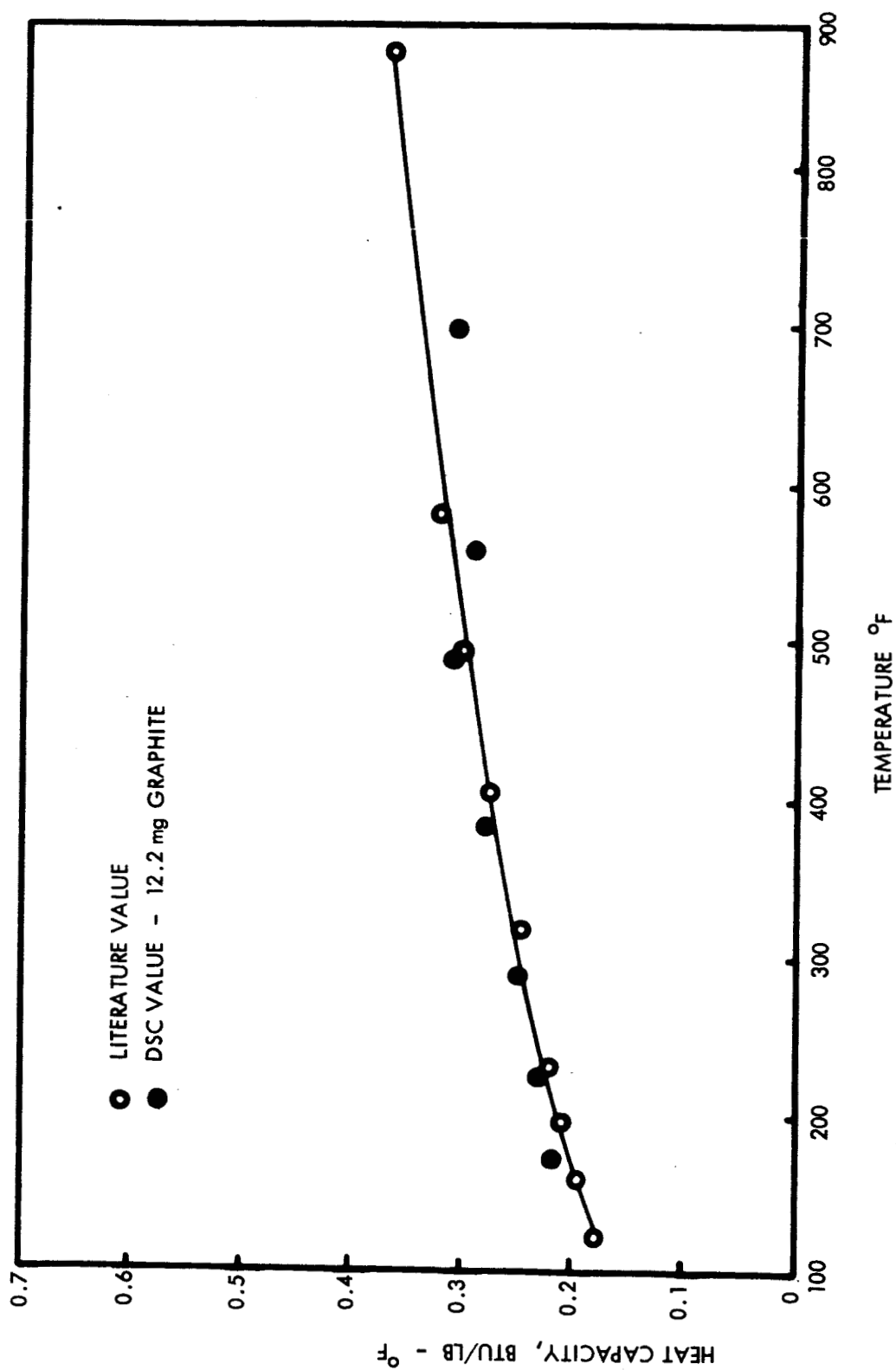


Figure 3.6 Astro Furnace and Calorimeter Assembly



latent heat of any transformation that may occur in the temperature range of ΔT .

If a second sample of heat capacity $C_2 W_2$ was substituted, then (if no transformation occurs in either sample so that latent heat may be omitted), by the use of the equation for the empty container ($H \times \Delta t_r = \Delta T_r \times C_r W_r$),

$$\frac{C_2 W_2}{C_1 W_1} = \frac{\frac{\Delta T_2}{\Delta t_2} - \frac{\Delta t_r}{\Delta T_r}}{\frac{\Delta t_1}{\Delta T_1} - \frac{\Delta t_r}{\Delta T_r}} \quad (3)$$

The quantity, $\frac{\Delta t}{\Delta T}$, is the slope of a time-temperature curve. In the equations above, the subscripts, r, 1 and 2 denote respectively this quantity for the empty container and for the container with specimens 1 and 2. The heat capacities of samples were thus directly proportional to the values of $\frac{\Delta t}{\Delta T}$ after they were corrected by subtracting a blank reading obtained from a heating or cooling curve of the container alone.

Experiments with each charred specimen were conducted over the temperature range from 630°F to 1710°F. Two separate series of measurements were made on each specimen and the average heat capacity values for the two series are reported in Section 5.2.2. The reproducibility of a given series was with few exceptions within $\pm 10\%$.

3.1.3 Preparation of Charred Specimens

Charred specimens were prepared from the virgin materials by heating the virgin specimens in a tube furnace under an atmosphere of flowing, high purity argon. All air was purged from the system prior to heating the sample. The samples were initially heated to approximately 1470°F, cooled to room temperature and weighed, and then reheated to 1400°F, cooled and

reweighed. A negligible weight change occurred between the first and second heating cycles. Table 3.1 shows a typical temperature vs. time profile used in preparing the char specimens. The weight changes occurring on charring are summarized in Table 3.2.

Figure 3.8 shows a photograph of charred specimens of each of the five ablative materials. The specimens were in the form of 0.75-inch diameter and 1.50-inch long cylinders. With the exception of the WBC 5217 material, which distorted rather severely, all of the charred specimens retained the shape and dimensions of the original virgin material samples rather well. Figure 3.9 shows a close-up photograph of the distorted WBC 5217 material (Mg(OH)_2).

Specimens charred in the above described manner were used both for heat capacity measurements and in determining char decomposition or melting temperature.

3.2 EXPERIMENTAL RESULTS

3.2.1 Heat Capacity Measurements on Virgin Ablative Materials

A summary of heat capacity data obtained on virgin ablative materials is presented in Table 3.3. These data are also plotted in Figures 3.10 and 3.11. The measurements taken at 441°F for all materials except the WBC 5217 are too high because of the initiation of decomposition of the resin system and the associated heat involved in this decomposition.

3.2.2 Heat Capacity Measurements on Charred Ablative Materials

Table 3.4 tabulates the results of the heat capacity measurements on charred samples of the five ablative materials. The test specimens were prepared as described in Section 3.1.3. The differential scan calorimeter (Section 3.1.1) was used for the lower temperature measurements and the modified Smith calorimeter (Section 3.1.2) was used for higher temperature measurements.

TABLE 3.1
TEMPERATURE TIME PROFILE FOR CHARRING
THE MX 2646 SPECIMEN

Time (min.)	Temperature (°F)
0	77
10	212
25	355
50	1070
80	1270
95	1310
105	1400
110	1440
120	1470
155	1460
170	1490
230	1490 ^a
290	400
320	200 ^b
335	390 ^c
345	695
375	1100
425	1390
465	1440 ^d

^aPower cut.

^bSample weighed at this point.

^cStart second heating cycle.

^dPower cut.

TABLE 3.2

WEIGHT LOSS ON CHARRING SPECIMENS FOR
HEAT CAPACITY MEASUREMENTS

Material	Virgin Material Weight/g	Char Weight, g	Percent Residue	Percent Weight Loss
MX 2646	19.577	16.434	83.9	16.1
WBC 2234	18.970	14.661	77.3	22.7
MX 2600	18.303	14.622	79.8	20.2
XR 2015	17.089	12.497	73.1	26.9
WBC 5217	20.913	12.705	60.7	39.3

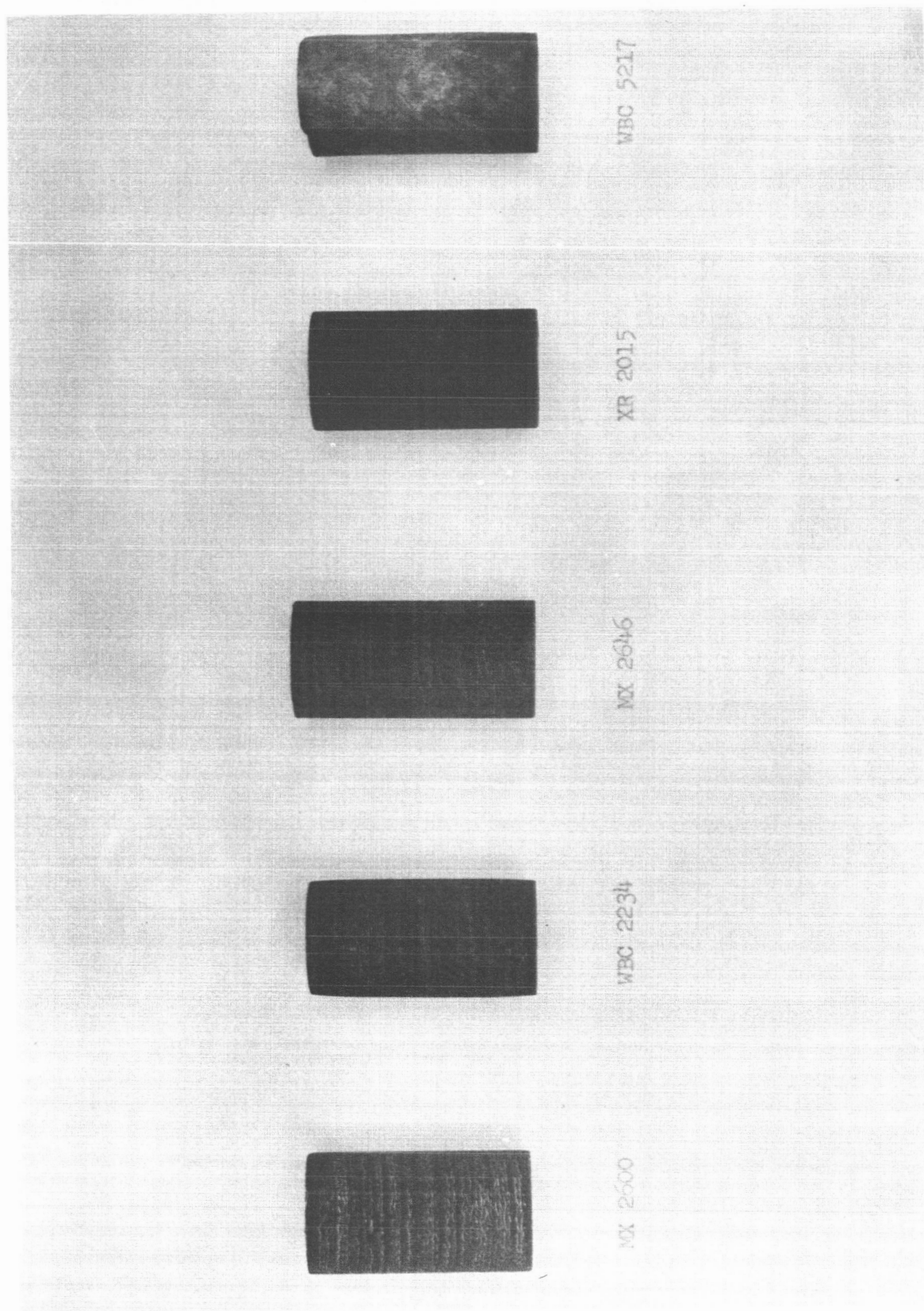


Figure 3. 8 Charred Ablative Specimens for Smith Calorimetry

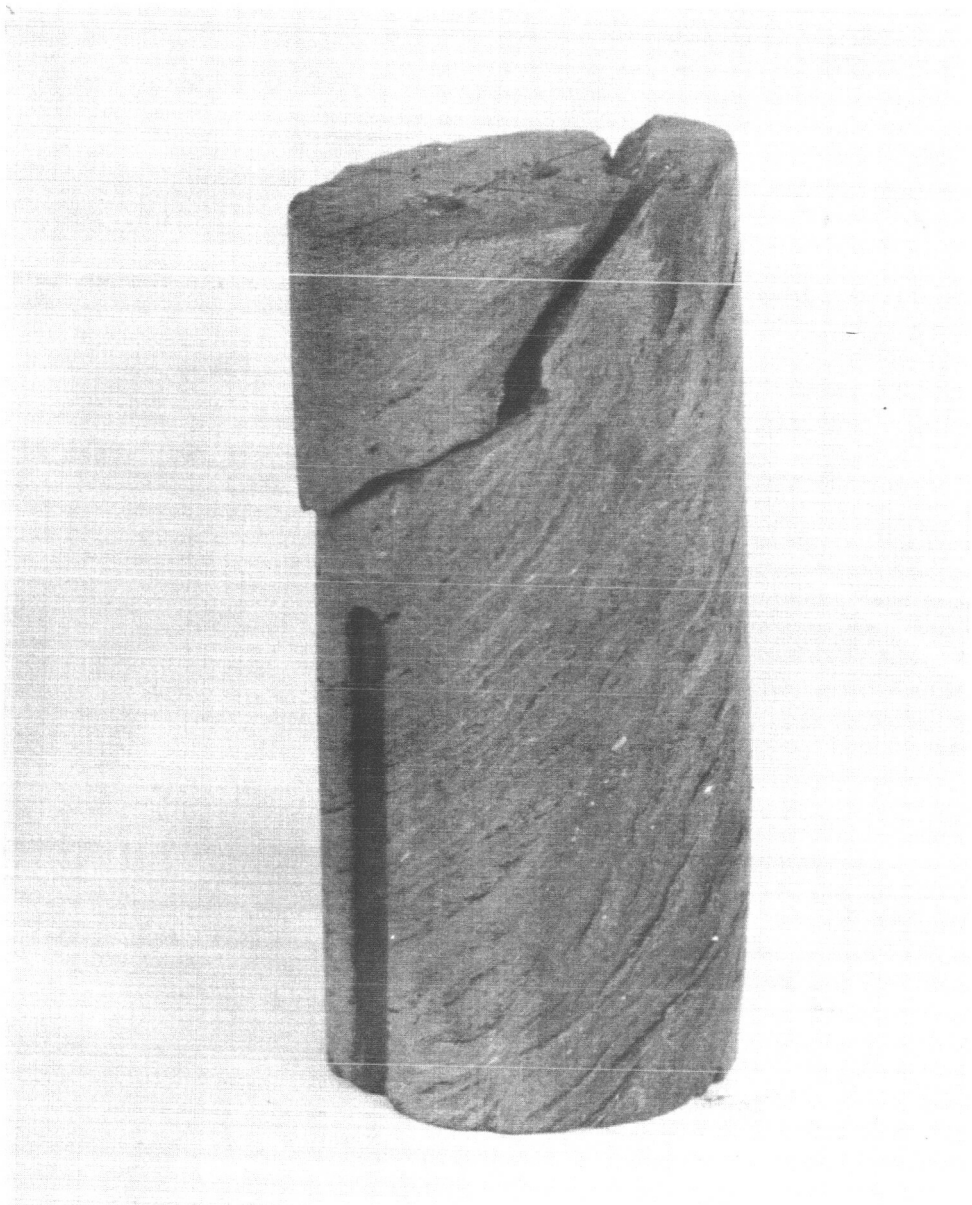


Figure 3.9 WBC 5217 Charred Ablative Specimen for
Smith Calorimetry

TABLE 3.3

SUMMARY OF HEAT CAPACITY MEASUREMENTS ON
VIRGIN ABLATIVE MATERIALS

Temperature °F	HEAT CAPACITY, BTU/lb-°F				
	XR 2015	MX 2600	MX 2646	WBC 2234	WBC 5217
126	0.29	0.26	0.25	0.24	0.32
180	0.30	0.27	0.26	0.26	-
216	0.30	0.26	0.26	0.26* 0.26	0.36
252	0.32	0.28	0.27	0.27	-
288	0.32	0.28* 0.28	0.27	0.27	-
324	0.33	0.28	0.28	0.27* 0.27	0.39
441	0.39	0.33	0.30	0.34	0.41

*Two readings were taken at this temperature.

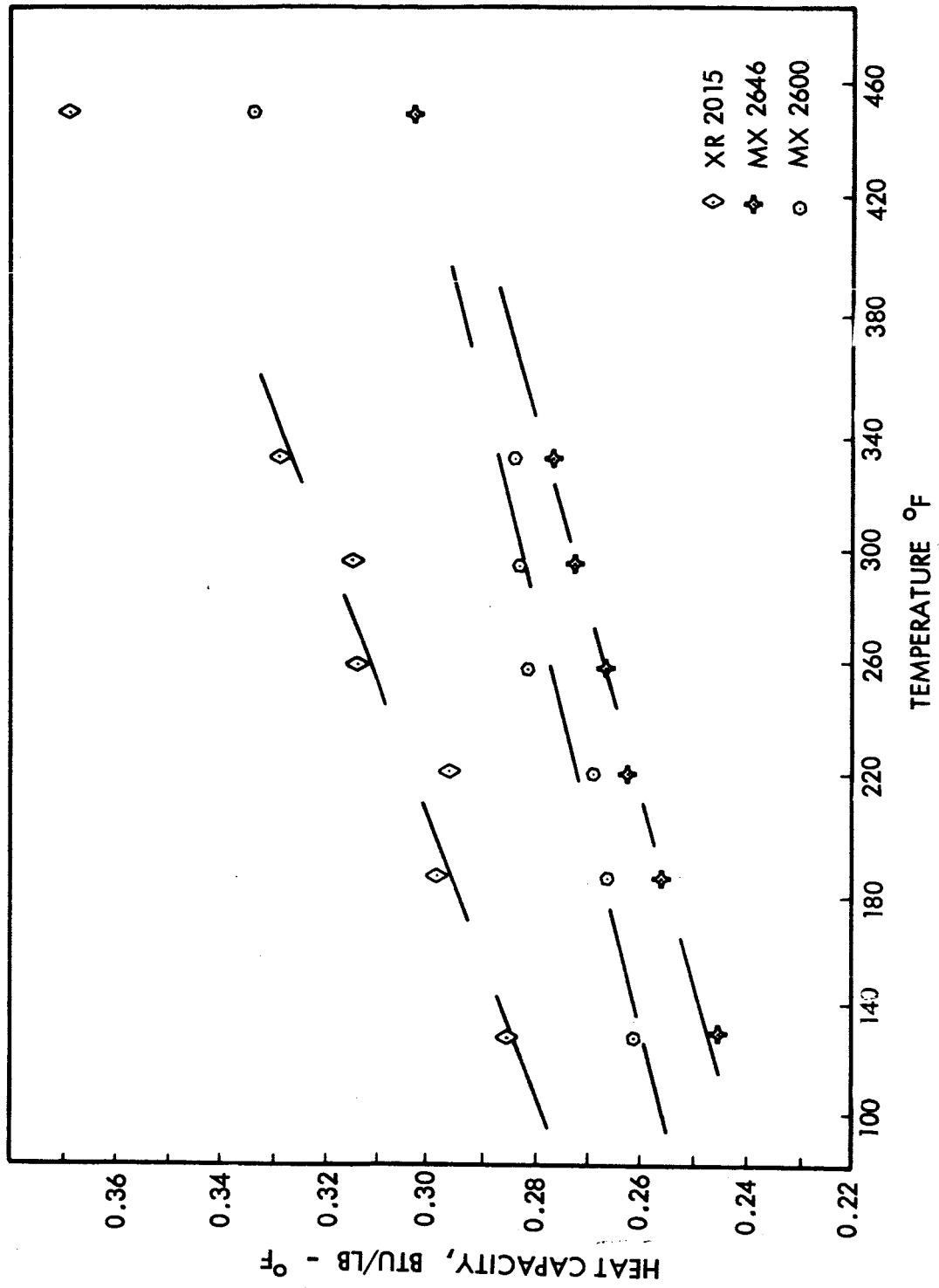


Figure 3.10 Heat Capacity as a Function of Temperature for Virgin Samples of XR 2015, MX 2646, and MX 2600

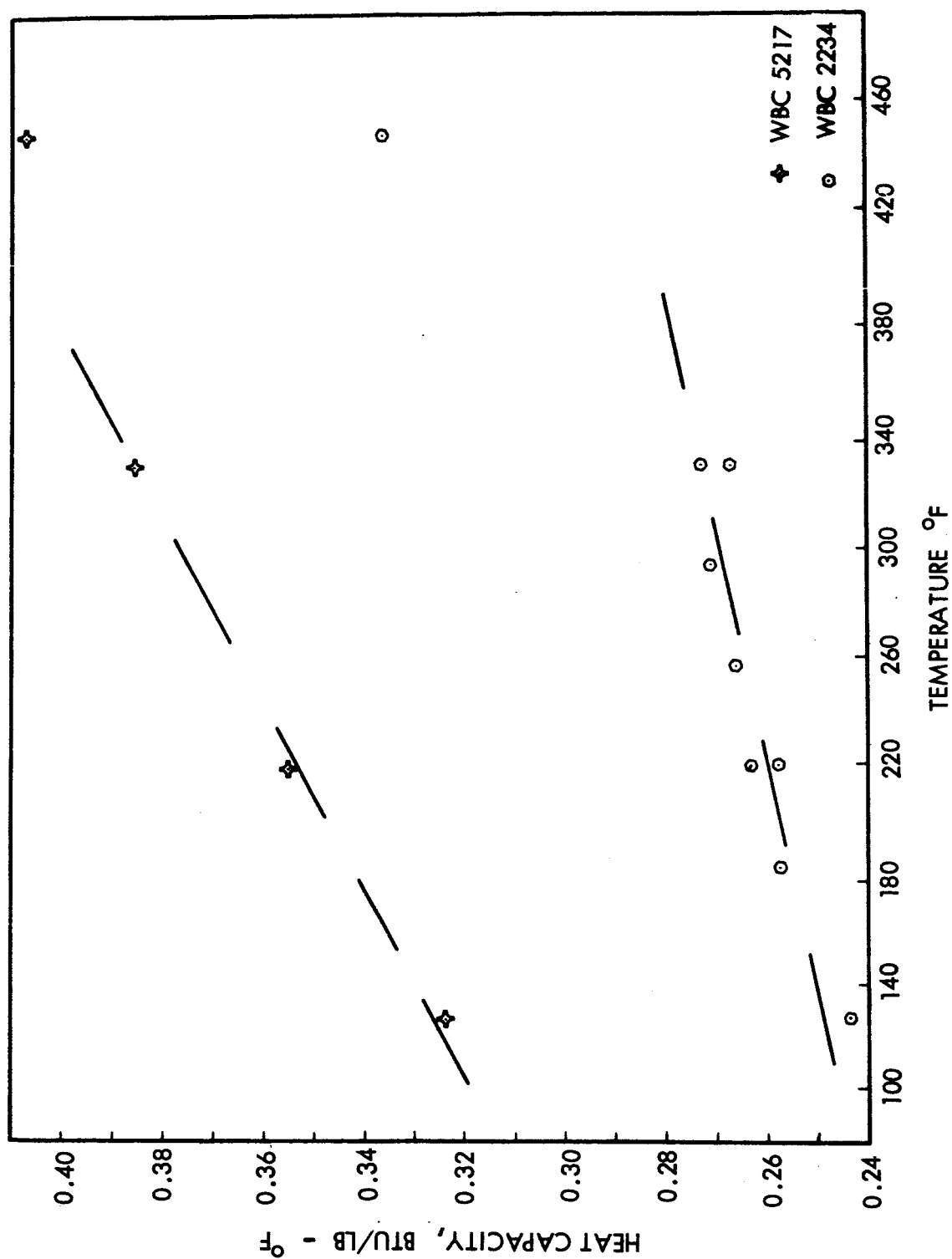


Figure 3.11 Heat Capacity as a Function of Temperature for Virgin Samples of WBC 5217, and WBC 2234

TABLE 3.4

HEAT CAPACITY MEASUREMENTS ON THE CHARRED
ABLATIVE MATERIALS

Temperature °F	HEAT CAPACITY, BTU/lb-°F				
	MX 2600	MX 2646	WBC 2234	XR 2015	WBC 5217
126 ^a	0.20	0.17	0.20	0.19	0.22
306 ^a	0.22	0.20	0.22	0.21	0.23
576 ^a	0.26	0.22	0.25	0.24	0.26
630 ^b	0.30	0.27	0.28	0.27	0.25
810 ^b	0.32	0.28	0.28	0.27	0.24
864 ^a	0.29	0.25	0.28	0.26	0.28
990 ^b	0.33	0.29	0.30	0.26	0.28
1170 ^b	0.37	0.29	0.33	0.29	0.28
1350 ^b	0.36	0.27	0.32	0.29	0.28
1530 ^b	0.33	0.29	0.29	0.30	0.28
1710 ^b	0.31	0.27	0.29	0.31	0.32

^aDifferential Scan Calorimeter Measurement

^bSmith Calorimeter Measurement

Figure 3.12 displays graphically the heat capacity data for the five charred specimens as a function of temperature. In the temperature region between 600°F and 900°F where both DSC measurements and Smith calorimeter measurements were made, the experimental data points for both types of measurements do not deviate from the best line through the data by more than $\pm 10\%$. Thus, there was rather good agreement between the measurements made with the differential scan calorimeter and the measurements made with the Smith calorimeter. In general, the Smith calorimeter data tended to be slightly higher than the DSC data.

3.3 RECOMMENDED HEAT CAPACITY DATA

Smooth curves have been drawn through the data points plotted in Figure 3.10, 3.11 and 3.12, and from these curves, tables of heat capacities recommended for use at specific temperatures have been generated. The recommended heat capacity data of virgin materials are listed in Table 3.5 and similar data for charred ablative materials are presented in Table 3.6. Heat capacities of the silica-carbon char were extrapolated between 1800°F and 3000°F by assuming no reaction between silica and carbon and applying additive corrections to the heat capacities of silica and carbon in relation to the chemical composition of the char. The chemical composition of the chars also presented in Table 3.6 was obtained by straight-forward calculation using the determined silica content (Table 2.2) and the determined silica and carbon residue (Table 3.2).

TABLE 3.5

RECOMMENDED HEAT CAPACITIES OF VIRGIN MATERIALS

Temperature, °F	Heat Capacity, BTU/lb - °F				
	MX 2600	MX 2646	WBC 2234	XR 2015	WBC 5217
100	0.25	0.24	0.24	0.28	0.32
200	0.27	0.26	0.26	0.30	0.34
300	0.28	0.27	0.27	0.32	0.38
400	0.30	0.28	0.28	0.34	0.41

TABLE 3.6
RECOMMENDED HEAT CAPACITIES OF CHARRED MATERIALS

Temperature, °F	Heat Capacity, BTU/lb - °F				
	MX 2600	MX 2646	WBC 2234	XR 2015	WBC 5217
200	0.21	0.18	0.21	0.21	0.23
400	0.25	0.22	0.24	0.23	0.25
600	0.27	0.24	0.26	0.25	0.26
800	0.30	0.26	0.29	0.26	0.27
1000	0.32	0.28	0.30	0.28	0.28
1200	0.34	0.28	0.31	0.29	0.28
1400	0.35	0.29	0.31	0.30	0.28
1600	0.33	0.30	0.31	0.31	0.29
1800	0.32 ^a	0.31 ^b	0.32 ^c	0.32 ^d	
2000	0.32 ^a	0.31 ^b	0.32 ^c	0.32 ^d	
2200	0.33 ^a	0.31 ^b	0.32 ^c	0.33 ^d	
2400	0.33 ^a	0.31 ^b	0.33 ^c	0.33 ^d	
2600	0.34 ^a	0.32 ^b	0.33 ^c	0.33 ^d	
2800	0.34 ^a	0.32 ^b	0.33 ^c	0.34 ^d	
3000	0.34 ^a	0.32 ^b	0.33 ^c	0.34 ^d	

- These data were calculated theoretically from determined composition of silica-carbon char and assuming no chemical reaction, MX 2600 - 82.2% SiO₂, 17.8%C.
- These data were calculated theoretically from determined composition of silica-carbon char and assuming no chemical reaction, MX 2646 - 91.3% SiO₂, 8.7%C.
- These data were calculated theoretically from determined composition of silica-carbon char and assuming no chemical reaction, WBC 2234 - 85.1% SiO₂, 14.9%C.
- These data were calculated theoretically from determined composition of silica-carbon char and assuming no chemical reaction, XR 2015 - 83.4% SiO₂, 16.6%C.

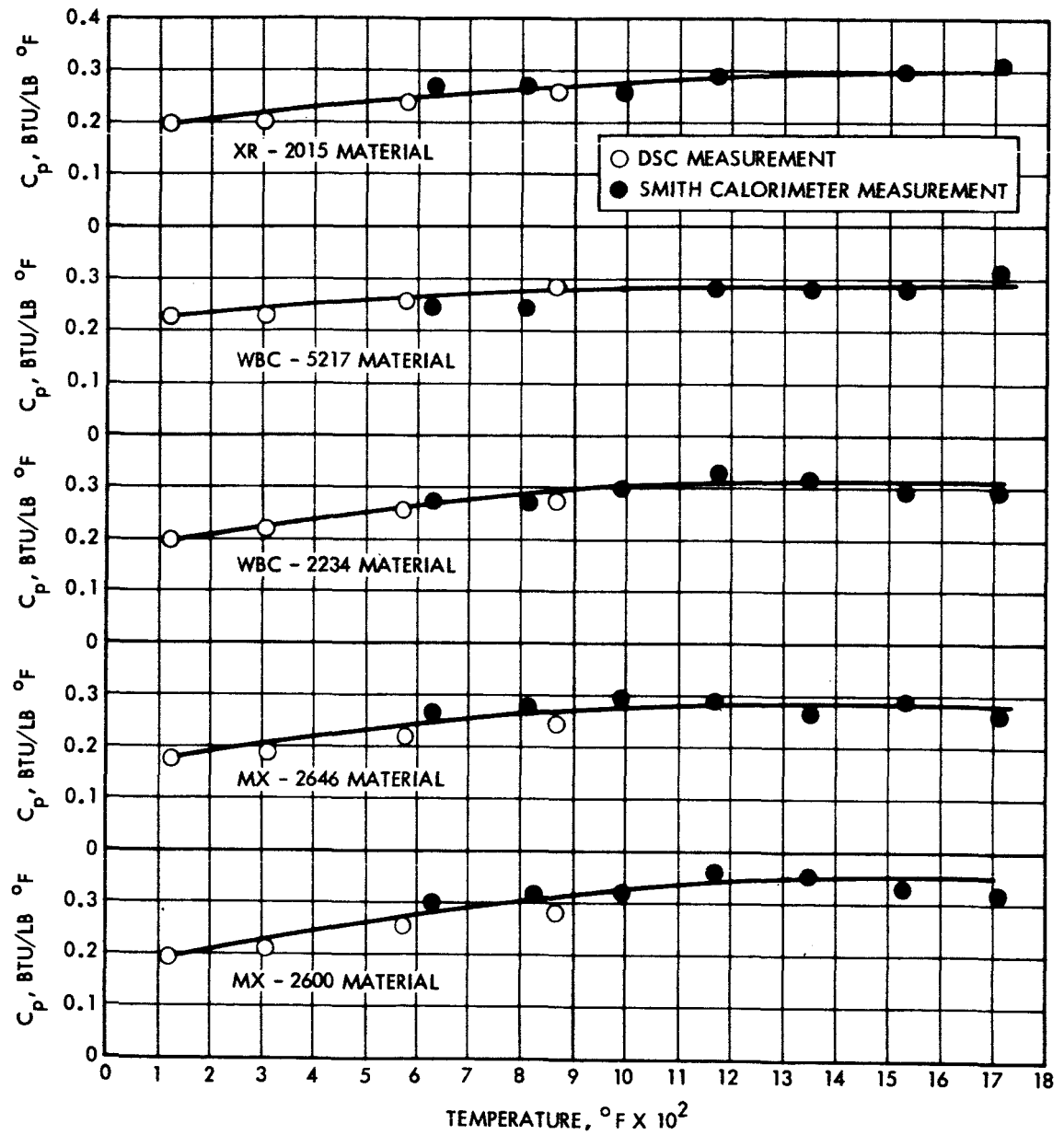


Figure 3.12 Heat Capacity vs. Temperature Data for the Five Charred Ablative Materials

4.0 BULK DENSITY MEASUREMENTS

Bulk density measurements in the temperature range from 77°F to 1652°F were conducted with 0.75-inch cube samples of each of the five ablative materials. In the following paragraphs, the experimental procedure is described and the results are presented.

4.1 EXPERIMENTAL PROCEDURE

The bulk density of each of the ablative samples was measured at four temperatures: 77°F, 392°F, 1112°F and 1652°F. Densities were computed on the basis of the weight of the sample after exposure for one hour to the experimental temperature and on the steady state volume of the sample at the experimental temperature. The volume of the samples at elevated temperatures was determined from post-temperature micrometer dimensions and the quantities a/a_0 and b/b_0 (the cathetometer measured ratio of dimensions at temperature to those after cooling). Because each material was composed of thin layers of flat sheets stacked one upon another, it was necessary to measure the linear expansion as a function of temperature in two dimensions for each sample: across the layer of flat sheets and along the plane of the individual sheets. It was assumed that the linear expansion of the flat sheets was the same for one dimension of the plan as for the other. This necessitated making two separate measurements on each type of material.

A typical measurement was made in the following manner:

The samples were weighed to the nearest 0.0001 gram on a Mettler single pan balance. Each of the three dimensions of the quasi-cube (nominal 0.75-inch on a side) was measured to ± 0.002 mm with a Starret metric micrometer. The samples were then placed in a high temperature quartz tube with an optically ground end piece and the tube was positioned in a Marion Electrical Company Hevi-Duty furnace. An optical cathetometer

was used to align the verticle dimension of the front surface of the sample, and an initial cathetometer measurement was made to the nearest 0.05 mm. Under a slow flow of Argon gas the sample was next heated to the experimental temperature and held at that temperature for one hour. A cathetometer measurement was than made and the sample was next cooled to room temperature. After the sample had cooled a final cathetometer reading was obtained. The sample was then removed from the furnace, reweighed, and its dimensions redetermined with the micrometer.

4.2 EXPERIMENTAL RESULTS

Tables 4.1 through 4.5 present the results of the bulk density measurements on each of the five ablative materials. The reported precision of the measurements are based on the precision of the individual cathetometer measurements. It is seen that the specimens in both the virgin material (77°F to 400°F) and the char region (1100°F to 1700°F) did not have constant weight. Additional weight may be lost if the heating period were increased beyond one hour. For this reason one concluded it is impossible to define a "virgin" or "charred" material state. Instead, a temperature region can be identified in which the material exists principally as the virgin material or charred material.

Figure 4.1 compares the bulk density vs. temperature data for the five ablative materials. As can be seen from this graph, the WBC 5217 and XR 2015 materials undergo the greatest change in density with increasing temperature. The dotted lines in Figure 4.1 show smooth curve transition between the bulk densities of the virgin and char material regions.

Figure 4.2 through 4.6 show photographs of samples of each of the five ablative materials both before heating and after heating to 1652°F . As can be seen from these photographs, all samples with the possible exception of the WBC 5217 material retained their shape and general dimensions very well.

TABLE 4.1
DENSITY MEASUREMENT DATA FOR MX 2600

TEMPERATURE °F	SAMPLE WEIGHT, g	DIMENSIONAL QUANTITIES			DENSITY	
		a/a ₀ *	b/b ₀ **	Volume, cc	g/cc	lb/ft ³
77	12.1781	1.000	1.000	7.070 ± 0.002	1.721 ± 0.001	107.8 ± 0.06
392	12.0718	1.01 ± 0.01	1.01 ± 0.01	7.27 ± 0.22	1.66 ± 0.05	103.7 ± 3.0
1112	10.3645	0.99 ± 0.01	1.00 ± 0.01	6.89 ± 0.21	1.51 ± 0.05	94.1 ± 3.3
1652	10.1715	1.01 ± 0.01	1.00 ± 0.01	6.71 ± 0.20	1.51 ± 0.05	94.1 ± 3.3

* With Grain (Ratio of dimensions at temperature to dimensions at 77 °F.)

** Against Grain.

TABLE 4.2
DENSITY MEASUREMENT DATA FOR MX 2646

TEMPERATURE °F	SAMPLE WEIGHT, g	DIMENSIONAL QUANTITIES			DENSITY	
		a/a _o *	b/b _o **	Volume, cc	g/cc	lb/ft ³
77	12.6405	1.000	1.000	7.043 ± 0.002	1.795 ± 0.001	112.1 ± 0.06
392	12.5620	1.01 ± 0.01	1.01 ± 0.01	7.19 ± 0.22	1.75 ± 0.05	109 ± 3.0
1112	10.6071	1.00 ± 0.01	1.00 ± 0.01	7.05 ± 0.21	1.51 ± 0.05	94.1 ± 3.3
1652	10.5186	1.01 ± 0.01	1.01 ± 0.01	7.14 ± 0.21	1.47 ± 0.04	91.4 ± 2.5

* With Grain (Ratio of dimensions at temperature to dimensions at 77 °F.)

** Across grain.

TABLE 4.3
DENSITY MEASUREMENT DATA FOR XR 2015

TEMPERATURE °F	SAMPLE WEIGHT, g	DIMENSIONAL QUANTITIES			DENSITY	
		a/a _o *	b/b _o **	Volume, cc	g/cc	lb/ft ³
77	10.1330	1.000	1.000	6.890 ± 0.002	1.471 ± 0.001	91.8 ± 0.06
392	9.7171	1.01 ± 0.01	1.02 ± 0.01	7.20 ± 0.22	1.35 ± 0.04	84.3 ± 2.5
1112	6.9720	1.00 ± 0.01	1.00 ± 0.01	6.84 ± 0.21	1.02 ± 0.03	63.5 ± 1.9
1652	6.8788	1.01 ± 0.01	1.00 ± 0.01	6.72 ± 0.20	1.02 ± 0.03	63.5 ± 1.9

* With grain (Ratio of dimensions at temperature to dimension at 77 °F.)

** Across grain.

TABLE 4.4
DENSITY MEASUREMENT DATA FOR WBC 2234

TEMPERATURE °F	SAMPLE WEIGHT, g	DIMENSIONAL QUANTITIES			DENSITY	
		a/a ₀ [*]	b/b ₀ ^{**}	Volume, cc	g/cc	lb/ft ³
77	12.1919	1.000	1.000	7.035 ± 0.002	1.733 ± 0.001	108.1 ± 0.06
392	11.7450	1.010 ± 0.01	1.003 ± 0.01	7.23 ± 0.24	1.62 ± 0.05	101.0 ± 3.1
1112	10.3227	1.008 ± 0.01	1.014 ± 0.01	6.97 ± 0.23	1.48 ± 0.05	92.4 ± 3.1
1652	10.0971	1.018 ± 0.01	1.016 ± 0.01	6.95 ± 0.23	1.45 ± 0.05	90.5 ± 3.1

* With grain (Ratio of dimensions at temperature to dimensions at 77 °F.)

** Across grain.

TABLE 4.5
DENSITY MEASUREMENT DATA FOR WBC 5217

TEMPERATURE °F	SAMPLE WEIGHT, g	DIMENSIONAL QUANTITIES			DENSITY	
		a/a _o [*]	Volume, cc	g/cc	lb/ft ³	
77	12.9615	1.000	6.924 ± 0.002	1.872 ± 0.001	117 ± 0.062	
392	12.7563	1.007 ± 0.01	7.01 ± 0.23	1.82 ± 0.06	113.7 ± 3.1	
1112	8.6395	1.014 ± 0.01	6.64 ± 0.22	1.30 ± 0.04	81.1 ± 2.5	
1652	7.9429	1.019 ± 0.01	6.58 ± 0.22	1.21 ± 0.04	75.6 ± 2.5	

* This sample had no grain structure; only one dimension measured.

a/a_o = ratio of dimension at temperature to dimension after cooling.

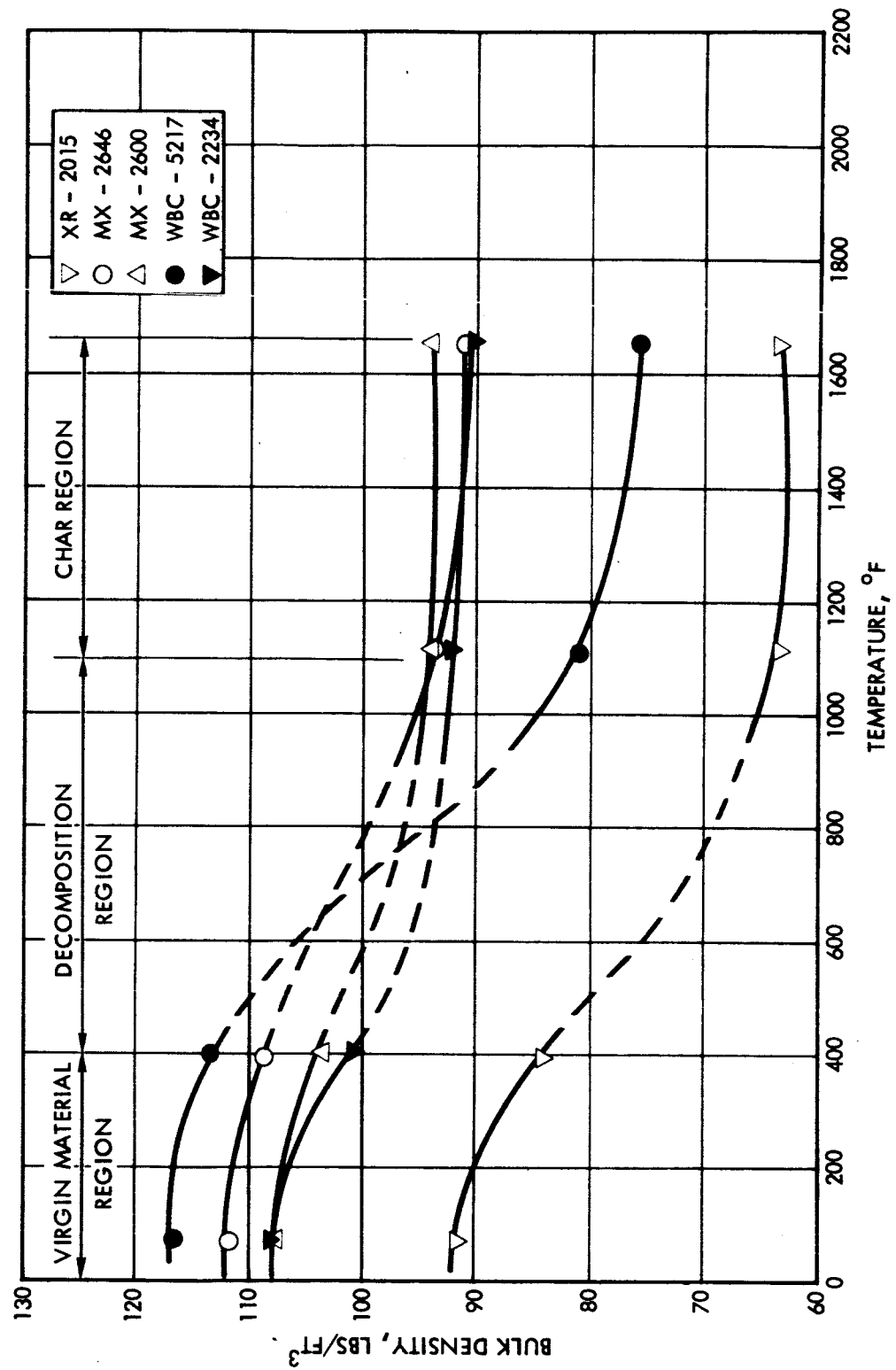


Figure 4.1 Steady State Bulk Density vs. Temperature Measurements for the Five Ablative Materials (All Samples 3/4 Inch Cubes)

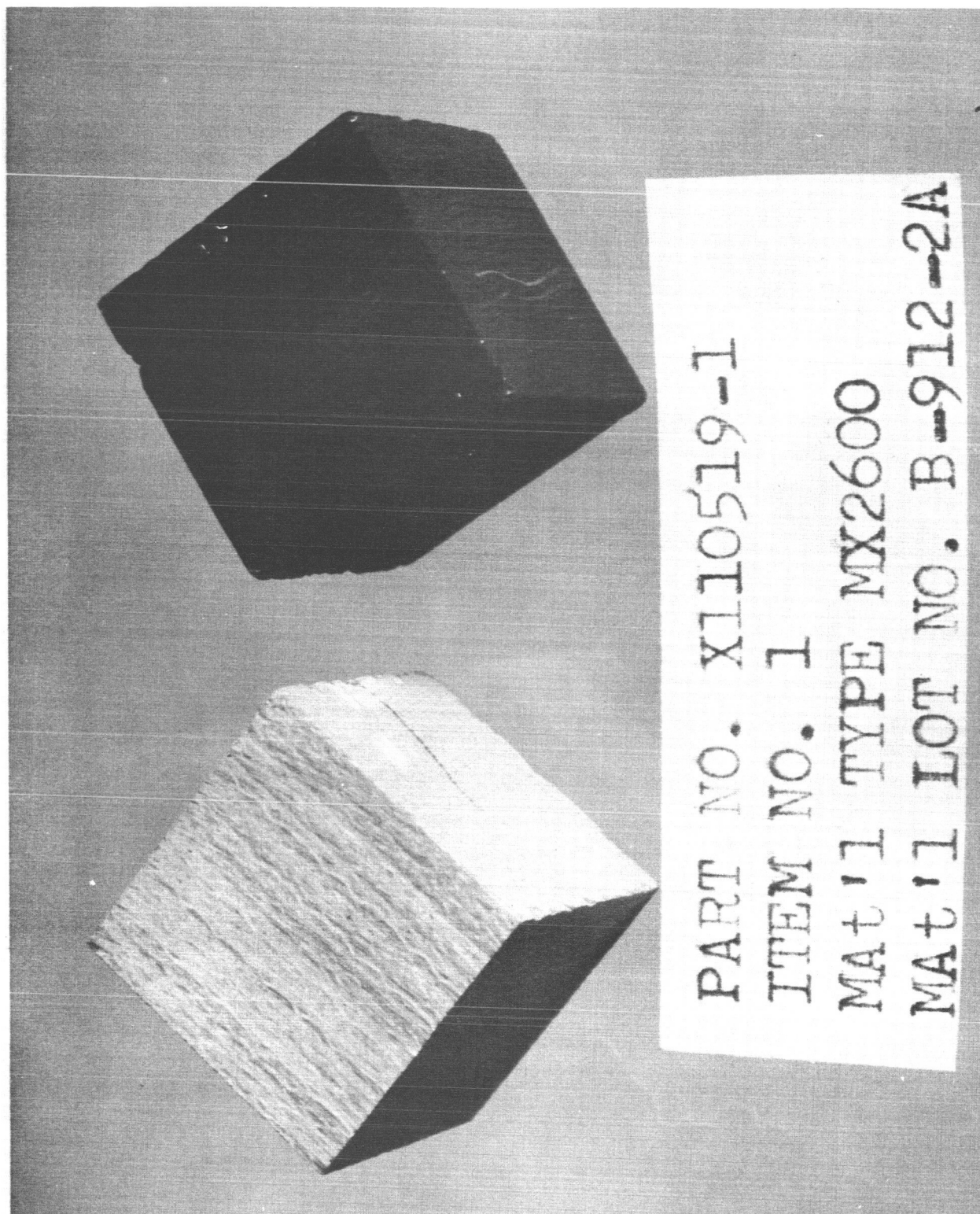


Figure 4.2 Photograph of MX 2600 Before (left) and After
(right) Heating to 1652°F

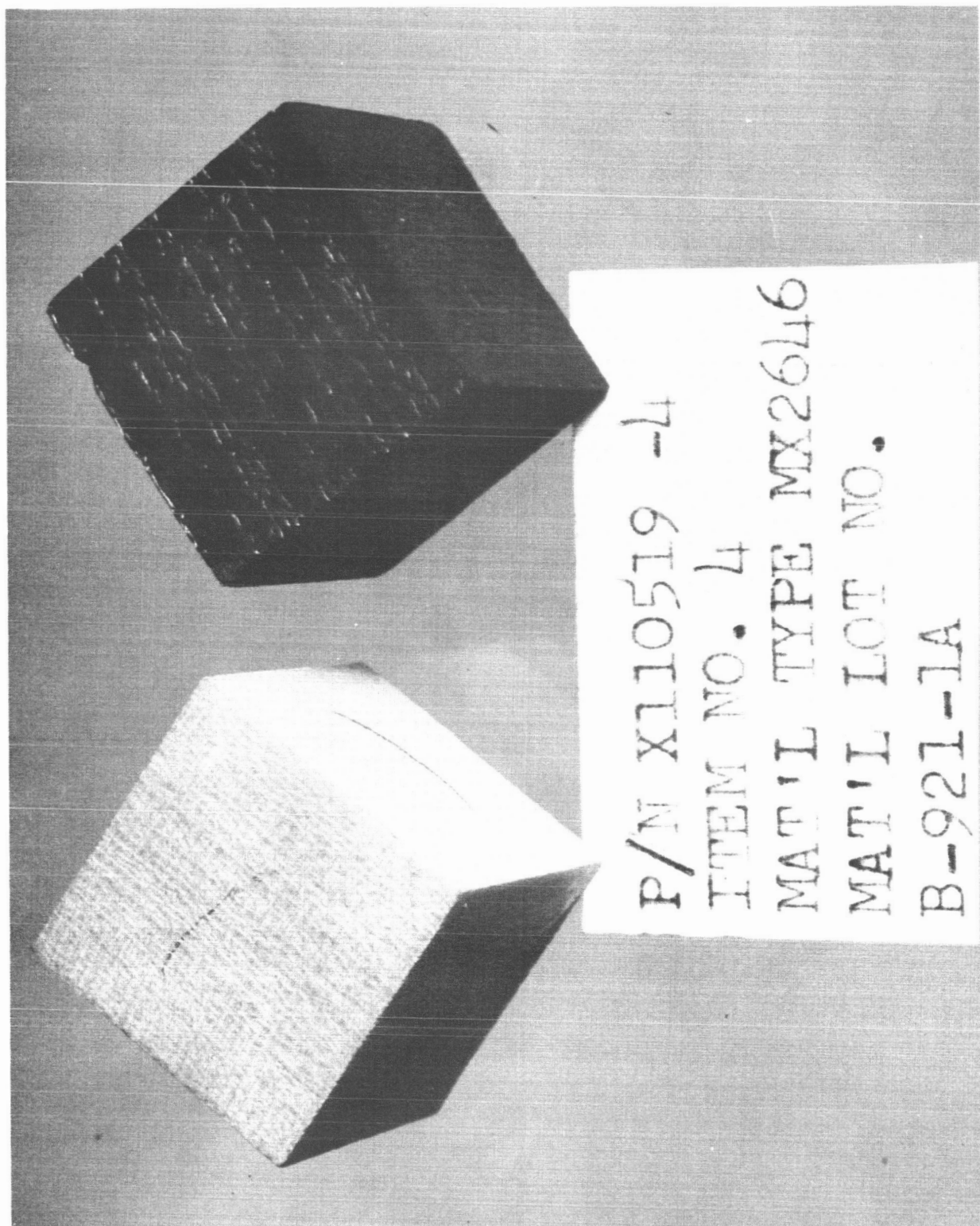


Figure 4.3 Photograph of MX 2646 Before (left) and After
(right) Heating to 1652°F

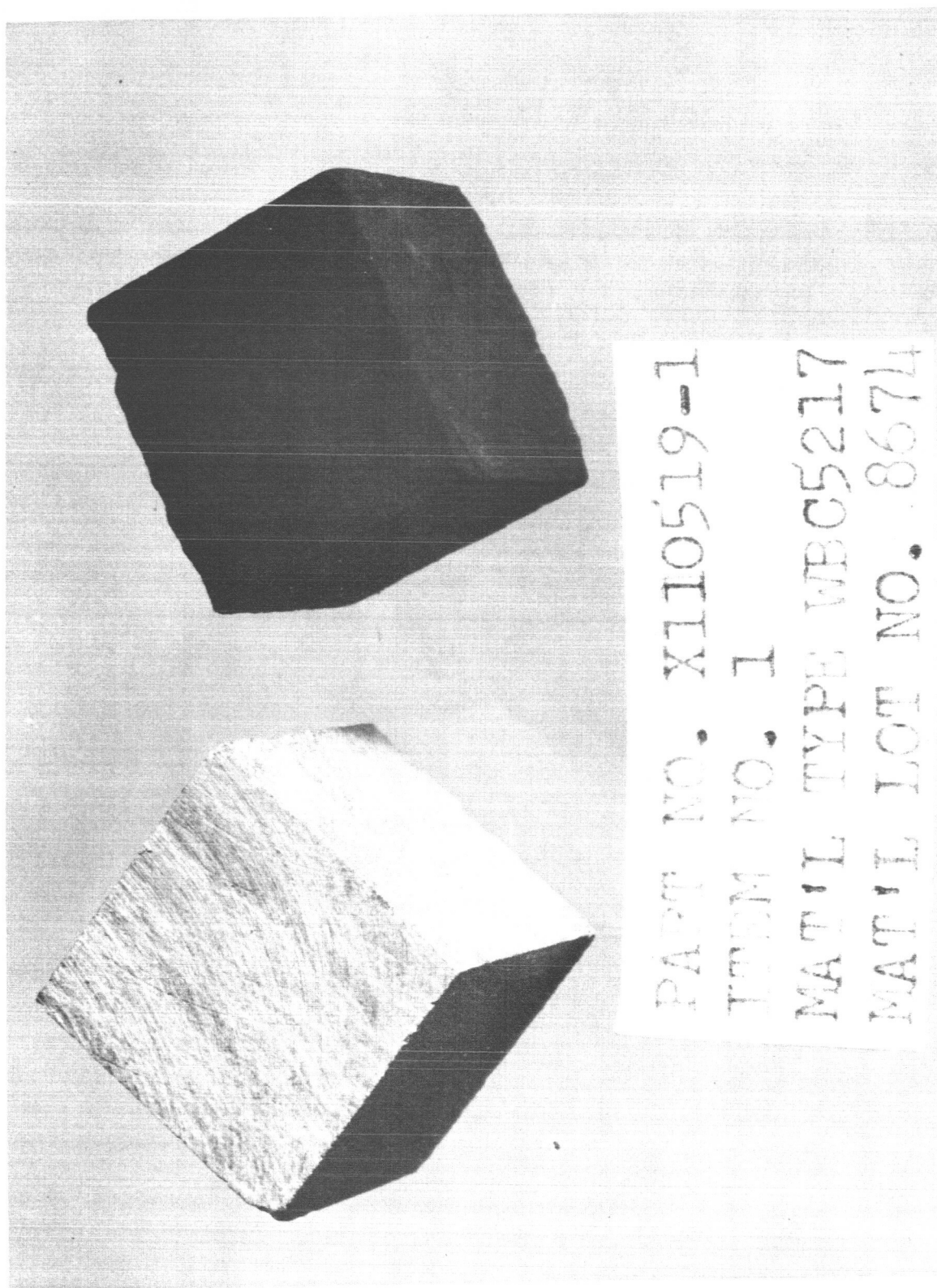


Figure 4.4 Photograph of WBC 5217 Before (left) and After
(right) Heating to 1652°F

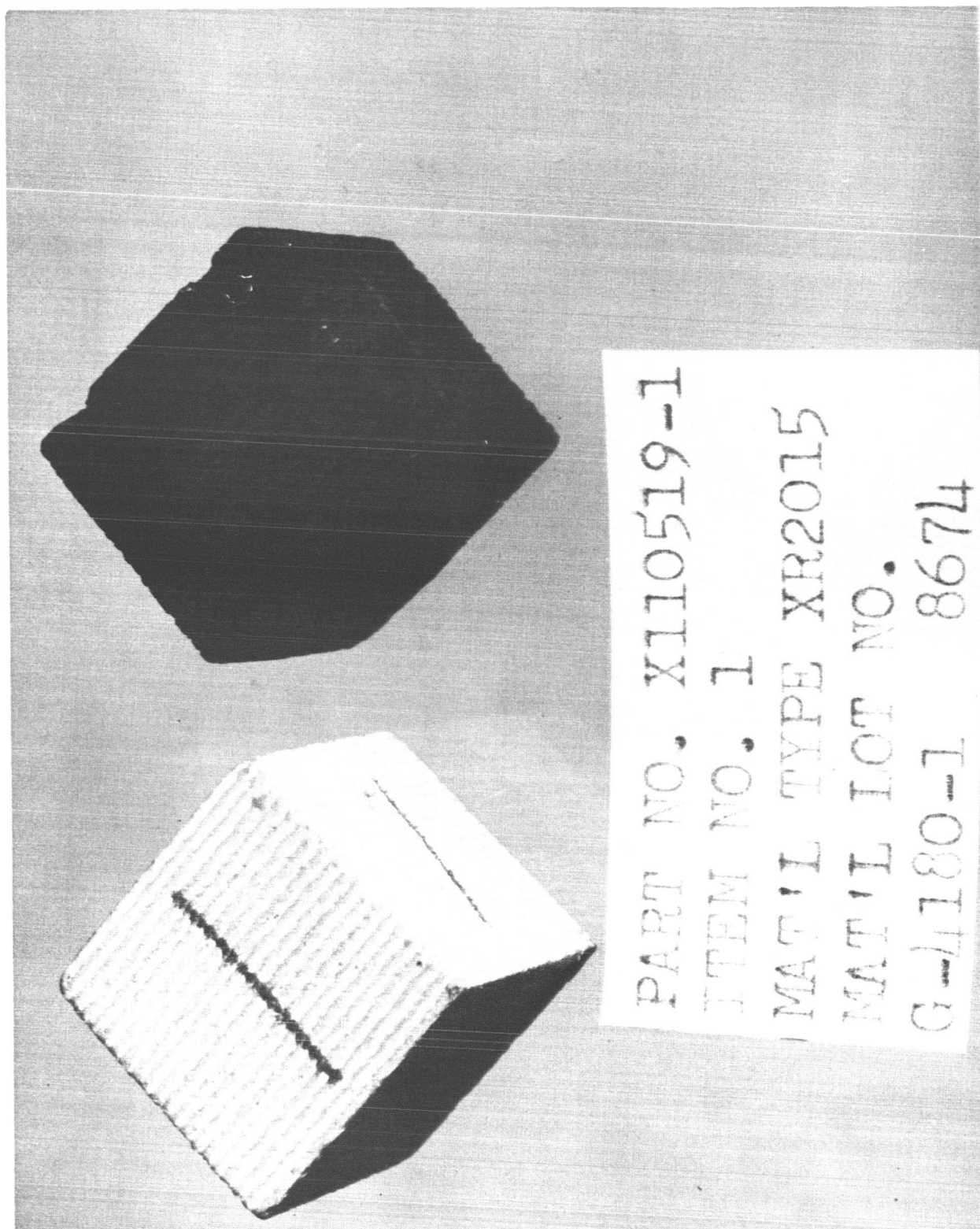


Figure 4.5 Photograph of XR 2015 Before (left) and After
(right) Heating to 1652°F

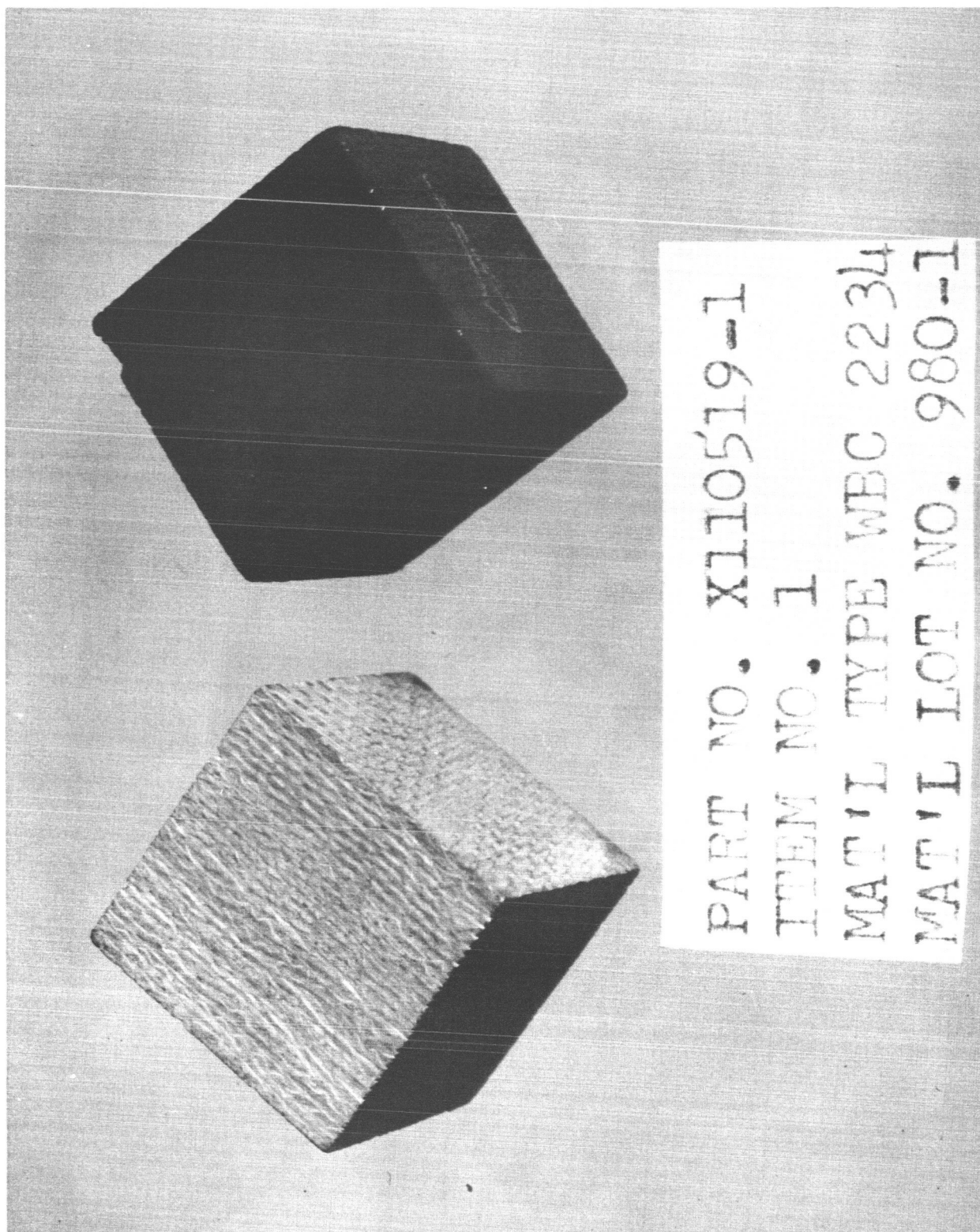


Figure 4.6 Photograph of WBC 2234 Before (left) and After
(right) Heating to 1652°F

5.0 RESIN DECOMPOSITION TEMPERATURE

The temperature at which the resin portion of the ablative material decomposed was determined using an Aminco Thermogravimetric balance. In this section of the report are presented a description of the operation of the thermogravimetric balance and the results of the tests on the five ablative materials.

5.1 OPERATION OF THE THERMOBALANCE

The Aminco Thermograv (Fig. 5.1) automatically records the weight of specimens as its temperature is increased (thermogravimetric analysis) in vacuum or controlled atmosphere. During this program, vacuum conditions were used for all tests. The weight of the specimen is recorded automatically as a function of temperature. The operation is described below:

The sample to be tested is placed in a crucible connected to and suspended beneath a transducer coil and a precision spring. Changes in sample weight cause an elongation or contraction of the spring resulting in a change in position of the armature with respect to the transducer. As a result, an electrical signal, proportional to the change in sample weight, is developed. This signal is demodulated and fed to the (Y) axis of the recorder. The input to the horizontal axis (X) is proportional time or temperature and together with the Y input furnishes the recorder with input to plot a curve weight vs. time or temperature.

Calculation of the weight retention at specific temperatures is determined by dividing the weight at specific temperatures by the weight of the original specimen. The resin decomposition temperature is often given as the mid point in the resultant S-shaped thermogravimetric curve. A temperature

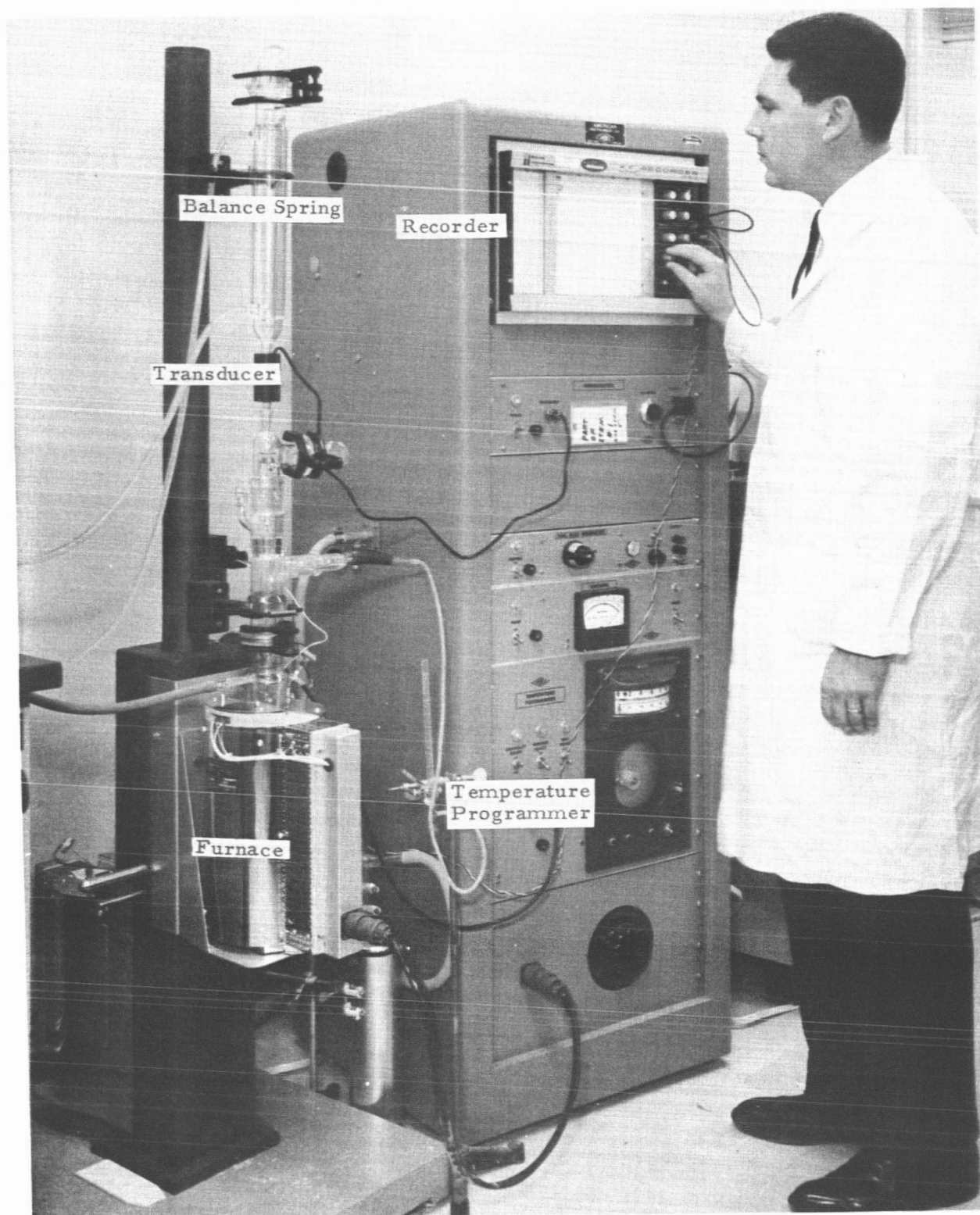


Figure 5.1 Aminco Thermograv

scanning rate of 5.4°F per minute was used throughout these experiments. This rate is accepted in the field of thermogravimetry as being slow enough to minimize the temperature lag between specimen and heater, yet not too slow to be impractical.

5.2 EXPERIMENTAL RESULTS

Thermograms of the ablative materials are shown in Figures 5.2 through 5.6. The percentage weight loss for these samples are presented in Table 5.1. The general shape of these curves is approximately the same, however, it is important to note that the WBC 5217 and XR 2015 have much higher percentage weight losses at elevated temperatures. The initial weight loss at low temperatures most likely arises from the loss of volatiles during post-cure of the virgin material. The high weight loss values for XR 2015 and WBC 5217 were expected from the gross changes in densities of these specimens observed previously (See Section 4.0). The WBC 5217 contains magnesium hydroxide which loses appreciable water content in this temperature region and hence explains the significant percent weight loss. The XR 2015 contains a modified elastomer phenylsilane resin system which explains its large percent weight loss in comparison with the other phenolic resin based materials.

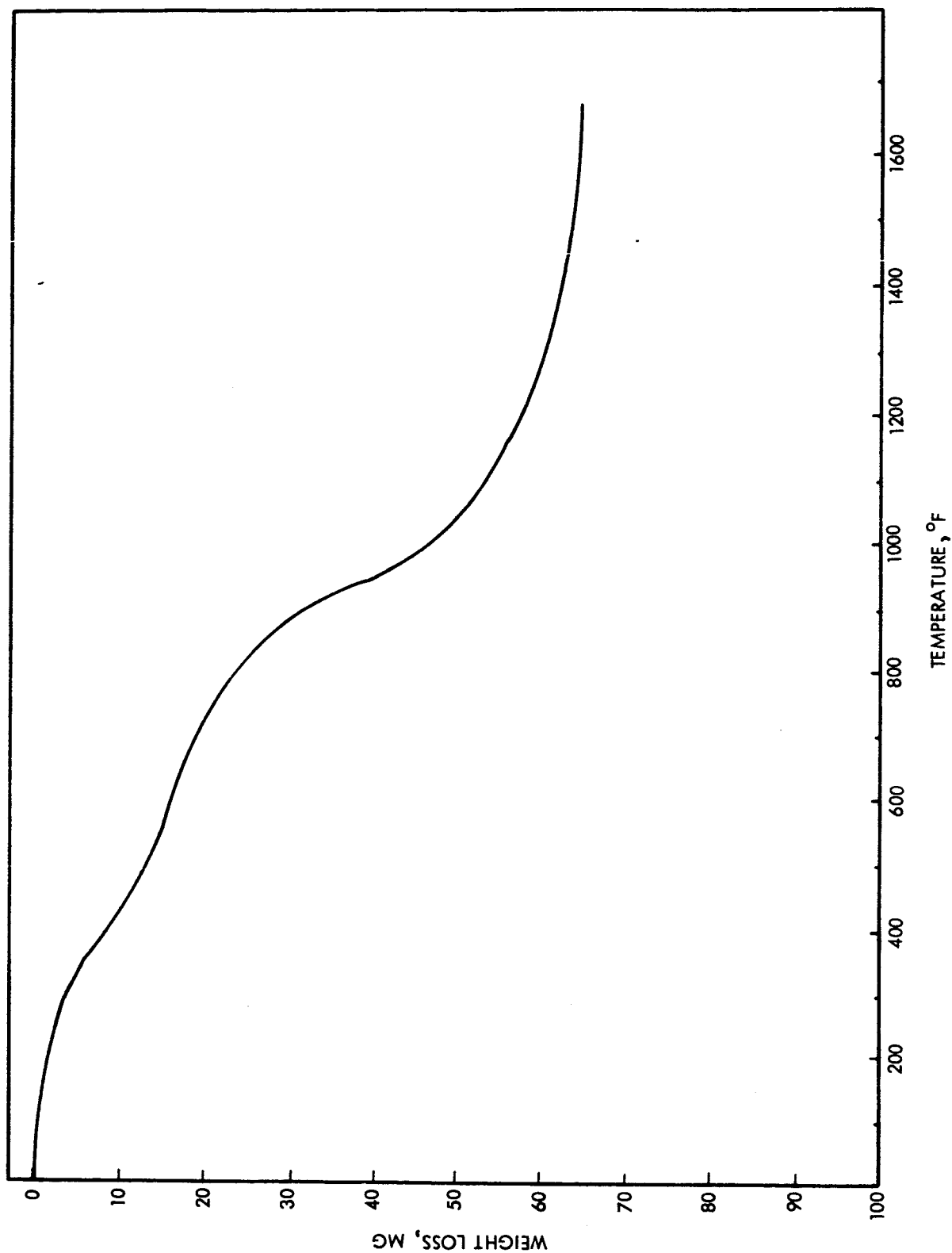


Figure 5.2 Thermogram of MX 2600
Environment: Vacuum; Scan Rate 5.4°F/min
Initial Weight: 421.7 mg

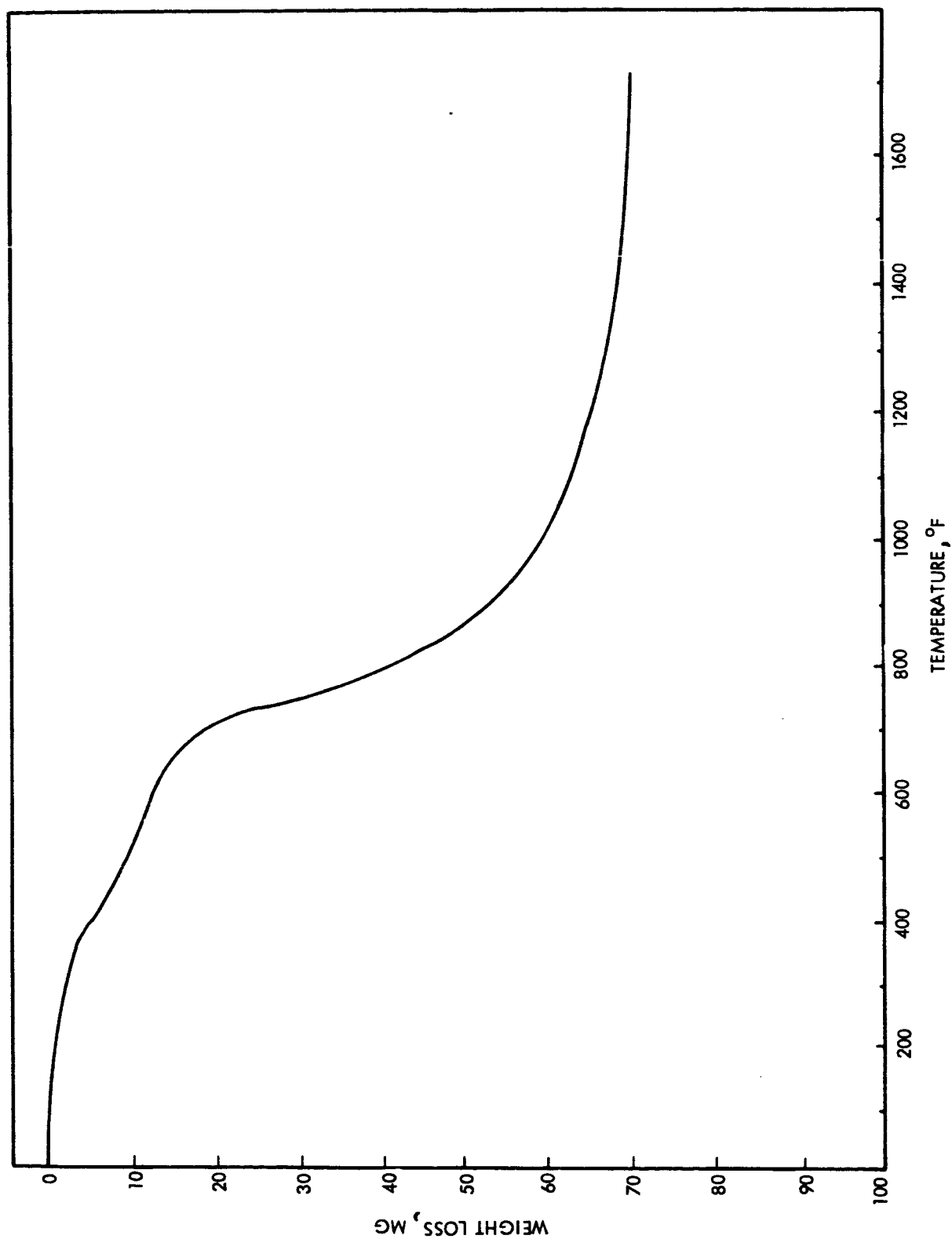


Figure 5.3 Thermogram of MX 2646
Environment: Vacuum, Scan Rate 5.4°F/min
Initial Weight: 423.2 mg

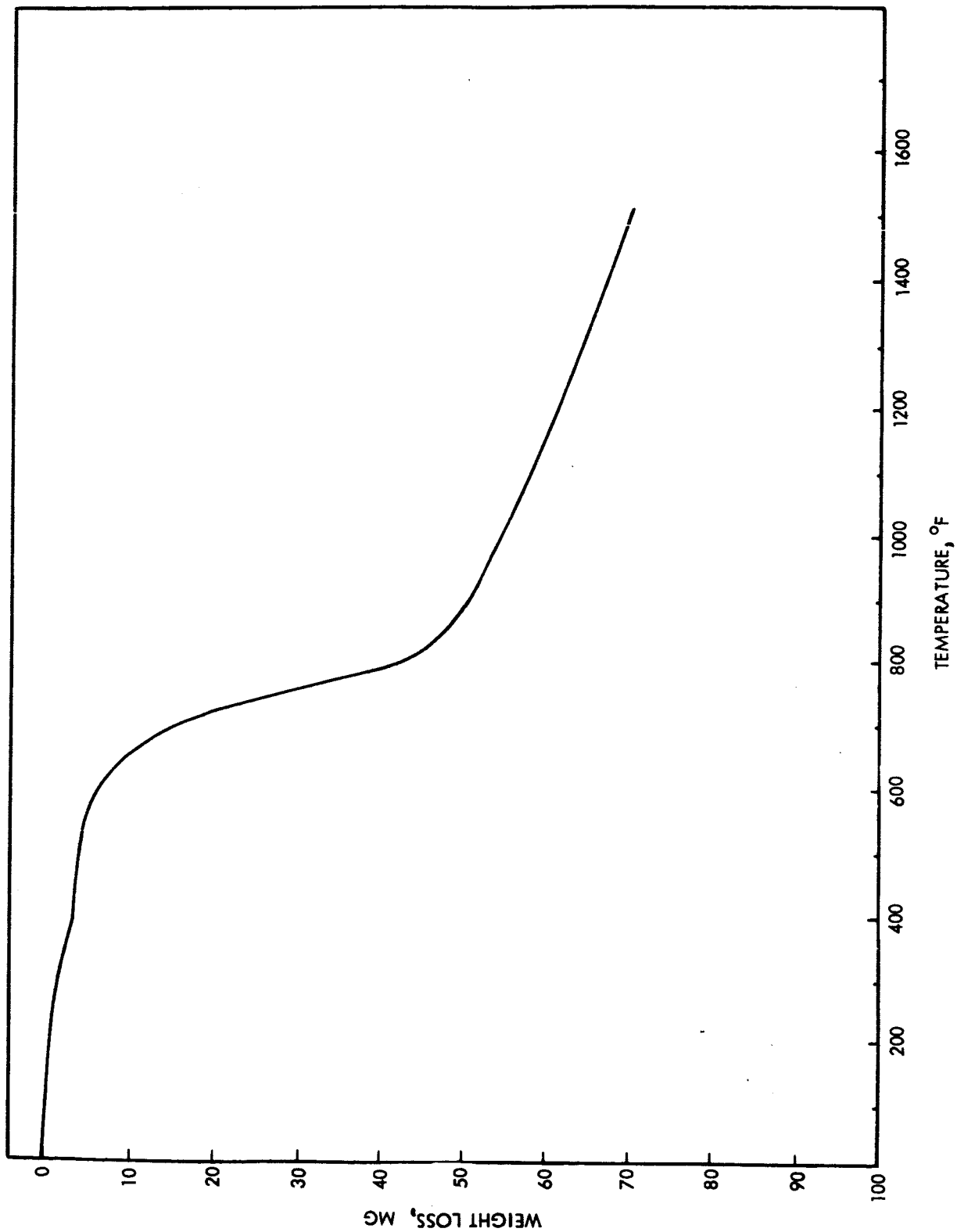


Figure 5.4 Thermogram of WBC 5217
Environment: Vacuum, Scan Rate 5.4°F/min
Initial Weight: 201.3 mg

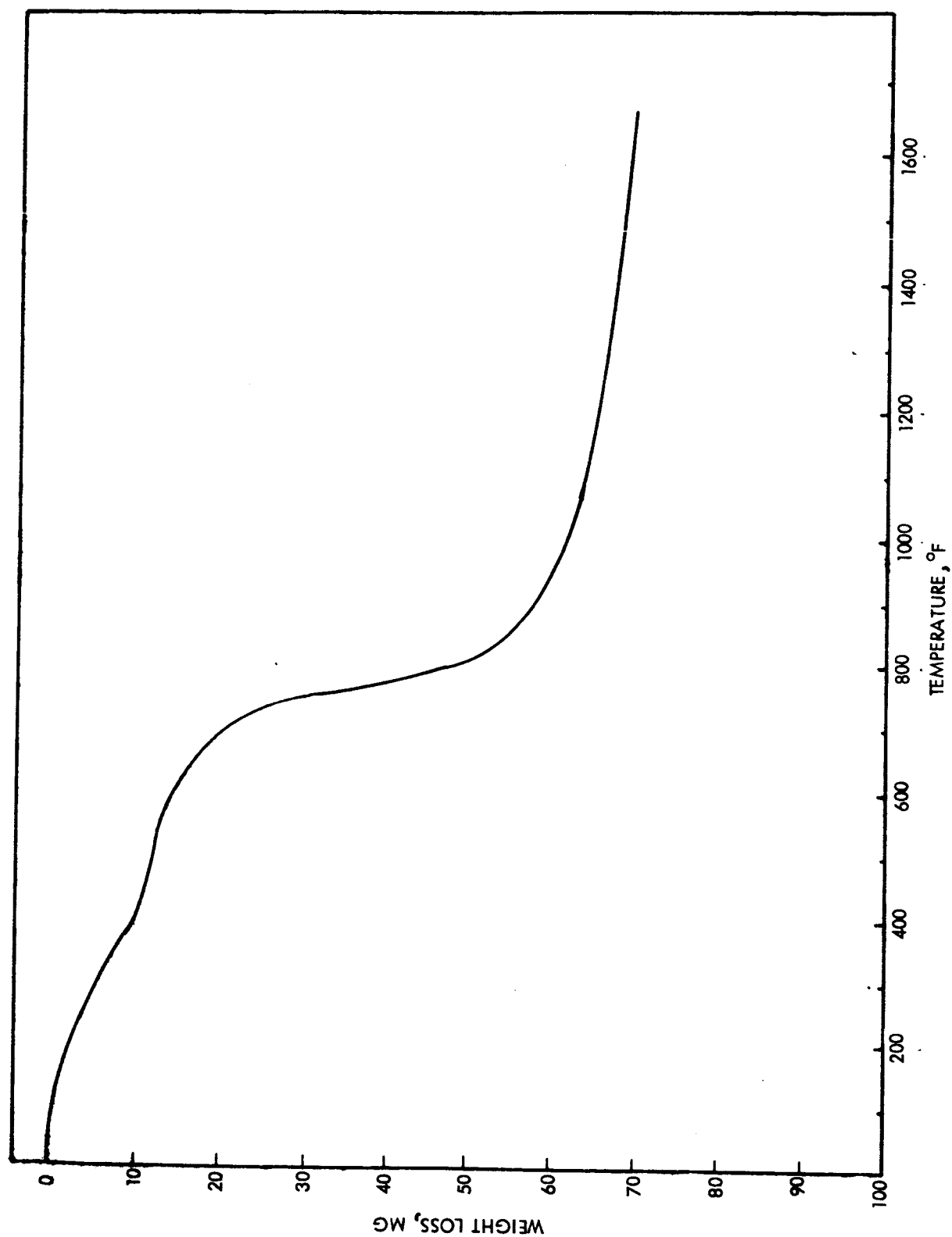


Figure 5.5 Thermogram of XR 2015
Environment: Vacuum; Scan Rate 5.4°F/min
Initial Weight: 216.0 mg

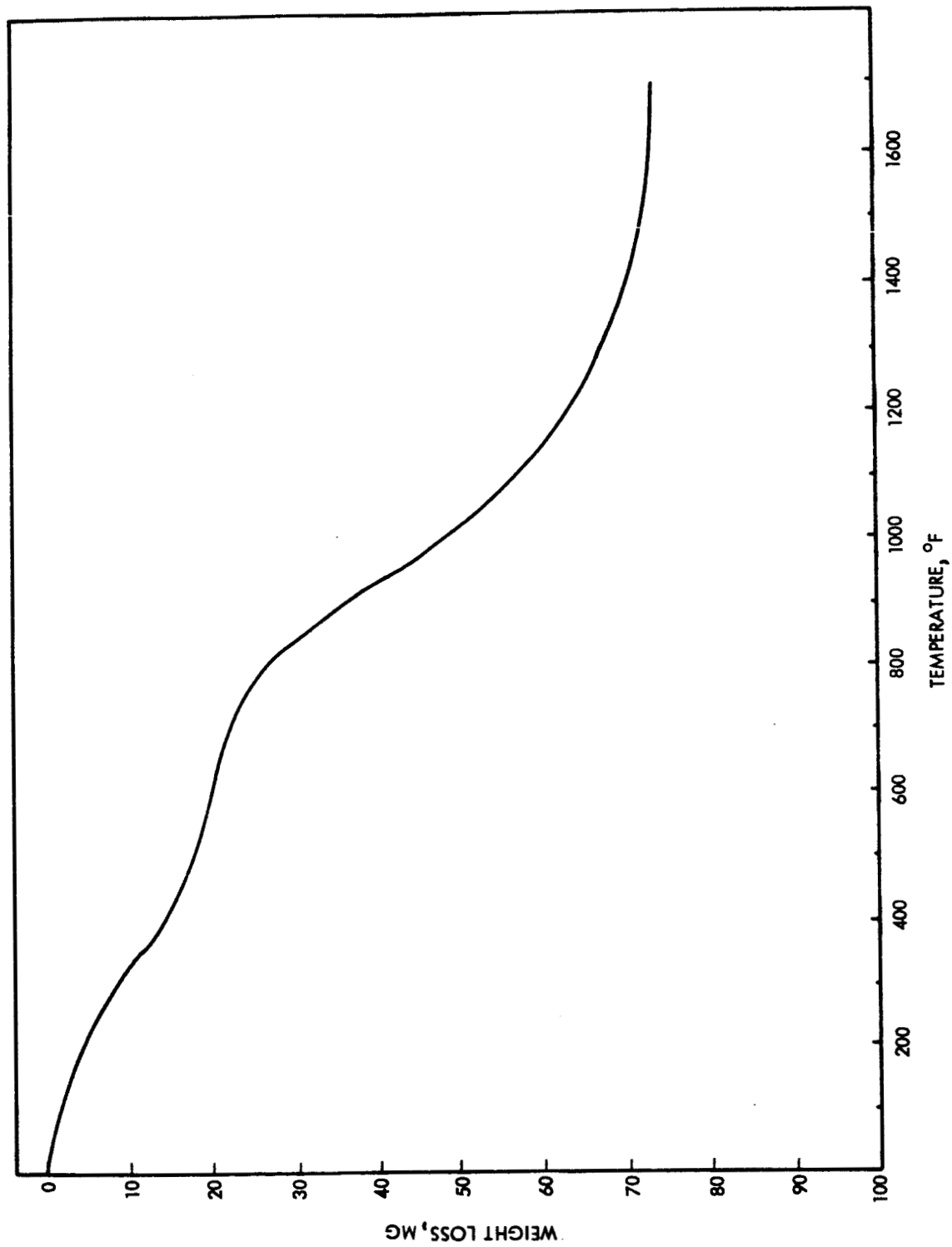


Figure 5.6 Thermogram of WBC 2234
Environment: Vacuum; Scan Rate 5.4°F/min
Initial Weight: 424.3 mg

TABLE 5.1
SUMMARY OF WEIGHT LOSS MEASUREMENTS
FOR THERMOGRAVIMETRIC ANALYSES OF ABLATIVE MATERIALS

Material	Temperature at Specified Percent Weight Loss, °F				Temperature at Mid-Point of S-Curve, °F	Total ^a Percent Loss
	3%	5%	8%	10%	12%	
MX 2600	485	730	915	960	1030	16.5
MX 2646	615	720	770	815	870	16.6
WBC 2234	375	610	895	950	1010	17.3
XR 2015 ^b	325	425	650	710	745	32.2
WBC 5217	565	655	705	720	735	^c

^a Percent weight loss of sample at level point approximately 1600°F.

^b Sample weight is approximately 200 milligrams compared to 400 milligrams for other samples.

^c Weight of the sample continues to decline appreciably after 1600°F.

6.0 MEASUREMENT OF CHAR MELTING AND DECOMPOSITION TEMPERATURES

The temperature at which charred specimens of each of the five ablative materials either formed a liquid phase or rapidly decomposed was measured in a tungsten ribbon melting point furnace. In addition, for the four materials which formed carbon-silica chars (MX 2600, MX 2646, WBC 2234, and XR 2015) measurements were made (in a temperature scan experiment) of the rate of carbon monoxide formation from the reaction of carbon with silica (e.g., $\text{SiO}_2 + \text{C} \rightarrow \text{SiO} + \text{CO}$). The experimental procedures and results are presented in the following paragraphs.

The original intent of the Phase I program was to measure only the melting temperature of the specimens in order to define the melting point of the materials for incorporation in thermal analysis models. However, previous experience at TRW had indicated that for the types of materials being evaluated the silica char reaction would proceed at very rapid rates above 2000°F . The experiments conducted on the four silica reinforced materials evaluated during this program were intended to determine the differences in the decomposition temperatures of the charred materials and point out the need for further investigations in this area. The inclusion of this phenomena in a thermal analysis model is particularly important when one considers the heat absorbed during the reaction is 24,000 BTU per pound of carbon consumed in the reaction.

6.1 CHAR MELTING EXPERIMENTS

Char melting experiments were conducted in an ultra high temperature tungsten ribbon melting point furnace. In this apparatus a small charred sample was slowly heated on a tungsten ribbon heating element under high vacuum (10^{-6} Torr). The sample temperature was measured with a micro-optical pyrometer and the sample was viewed through a pyrometer telescope from a distance of approximately six inches. The initial formation of a molten

phase could readily be observed. The reported specimen (brightness) temperature are the black body temperature. No correction was made for the emissivity of the specimen. However, if the specimen were considered to have an emissivity of 0.7 then a correction of +278°F and +322°F would be realized at observed brightness temperatures of 2500°F and 3000°F respectively. Presently the emissivity of the charred specimens is not known accurately, however measurements which are being conducted under a separate phase of the program will provide the necessary data such that the temperatures presented herein may be properly corrected. The formula for correction of the temperature is

$$T_c = (\epsilon^{-1/4} - 1) (T_b + 460) ,$$

where

T_c = temperature correction to be added to the reported brightness temperature,

ϵ = emissivity of the test specimen,

T_b = the reported brightness temperature, °F

In addition, to the observed melt temperature, an indication of the silica-carbon reaction was obtained by noting the system pressure rise since carbon monoxide is evolved when carbon reacts with silica (e. g., $\text{SiO}_2 + \text{C} = \text{SiO} + \text{CO}$).

Tables 6.1 through 6.5 present the results and observations of the experiments with five charred ablative materials.

The specimens which were utilized in these experiments were the charred samples previously used in the high temperature heat capacity experiments.

TABLE 6.1
CHARRED MX 2600 MELTING EXPERIMENT

TEMPERATURE (Brightness)	OBSERVATION
2200°F	System pressure rise indicating silica-carbon reaction initiated.
2500°F	A bright zone was evident on one part of the sample; perhaps indicating the initiation of a very viscous molten phase.
2750°F	Liquid phase definitely evident.
2800°F	Bubbling in the molten mass, indicating rapid evolution of gases (e. g. , CO) from fast reaction between carbon and silica; rapid system pressure rise.
3050°F	Rapid bubbling.

TABLE 6. 2
CHARRED XR 2015 MELTING EXPERIMENT

TEMPERATURE (Brightness)	OBSERVATION
2400°F	Some of the fibers appeared to be softening.
2900°F	Individual fibers fused; system pressure rise, indicating some reaction.
3200°F	Nearly all fibers had melted.

TABLE 6. 3
CHARRED MX 2646 MELTING EXPERIMENT

TEMPERATURE (Brightness)	OBSERVATION
2460°F	Molten phase formed; pressure rise, indicating silica-carbon reaction.
3000°F	Steep pressure rise, indicating rapid reaction.
3200°F	Vigorous bubbling within the molten sample; a portion of the sample moved away from the heating element.

TABLE 6. 4

CHARRED WBC 2234 MELTING EXPERIMENT

TEMPERATURE (Brightness)	OBSERVATION
2360°F	Formation of a viscous molten phase.
2640°F	Pressure rise, indicating rapid carbon-silica reaction.
3170°F	Rapid bubbling in molten phase, indicating very fast reaction.

TABLE 6. 5

CHARRED WBC 5217 MELTING EXPERIMENT

TEMPERATURE (Brightness)	OBSERVATION
2720°F	Pressure rise, indicating reaction taking place.
2820°F	Rapid bubbling and volatilization of material.
3000°F	Rapid loss of material from volatilization.

6.2 TEMPERATURE SCAN EXPERIMENTS

A high temperature, constant volume, reaction kinetics systems was utilized for cursory temperature scan experiments with charred samples of the four ablative materials which formed carbon-silica chars (MX 2600, MX 2646, WBC 2234, and XR 2015). In these experiments a sample of charred material was slowly heated in a preevacuated, constant volume apparatus and the sample temperature and system pressure rise (due to carbon monoxide formation from the reaction $\text{SiO}_2 + \text{C} \rightarrow \text{SiO} + \text{CO}$) were continually recorded as a function of time. Figure 6.1 shows a schematic diagram of the apparatus.

Figures 6.2 through 6.5 show the results of the temperature scan experiments. The graphs present the temperature vs. time and carbon monoxide pressure vs. time curves for experiments with each of the four char specimens. It is apparent from these graphs that all four of the charred materials rapidly decompose in the 2300 to 2500°F temperature region.

It is important to note that these experiments are cursory in nature and serve only to show the temperature at which the reaction proceeds at an appreciable rate. Controlled temperature scan and isothermal experiments in which the pressure is monitored provides a means for determination of reaction rates and activation energies of the char decomposition reactions.

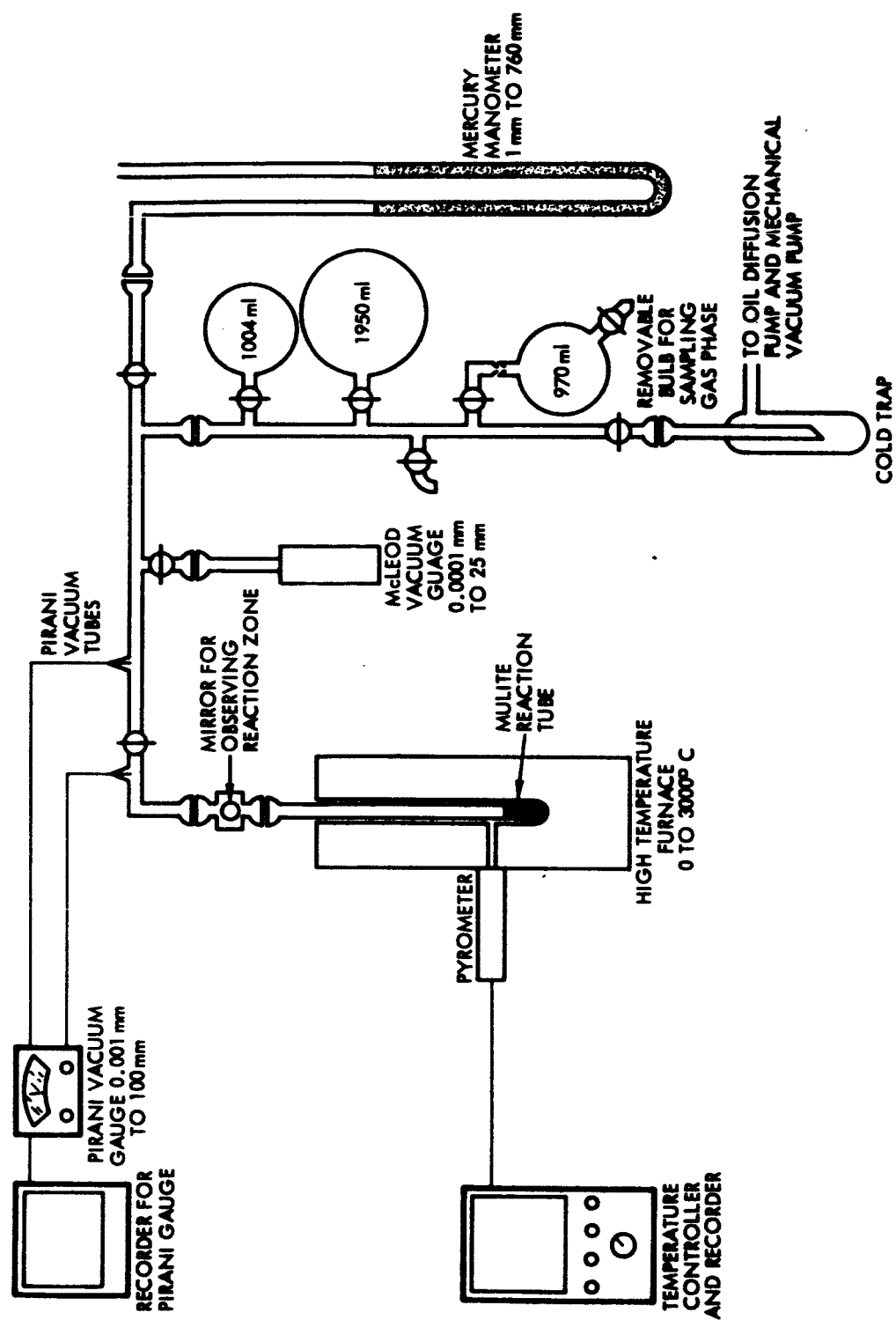
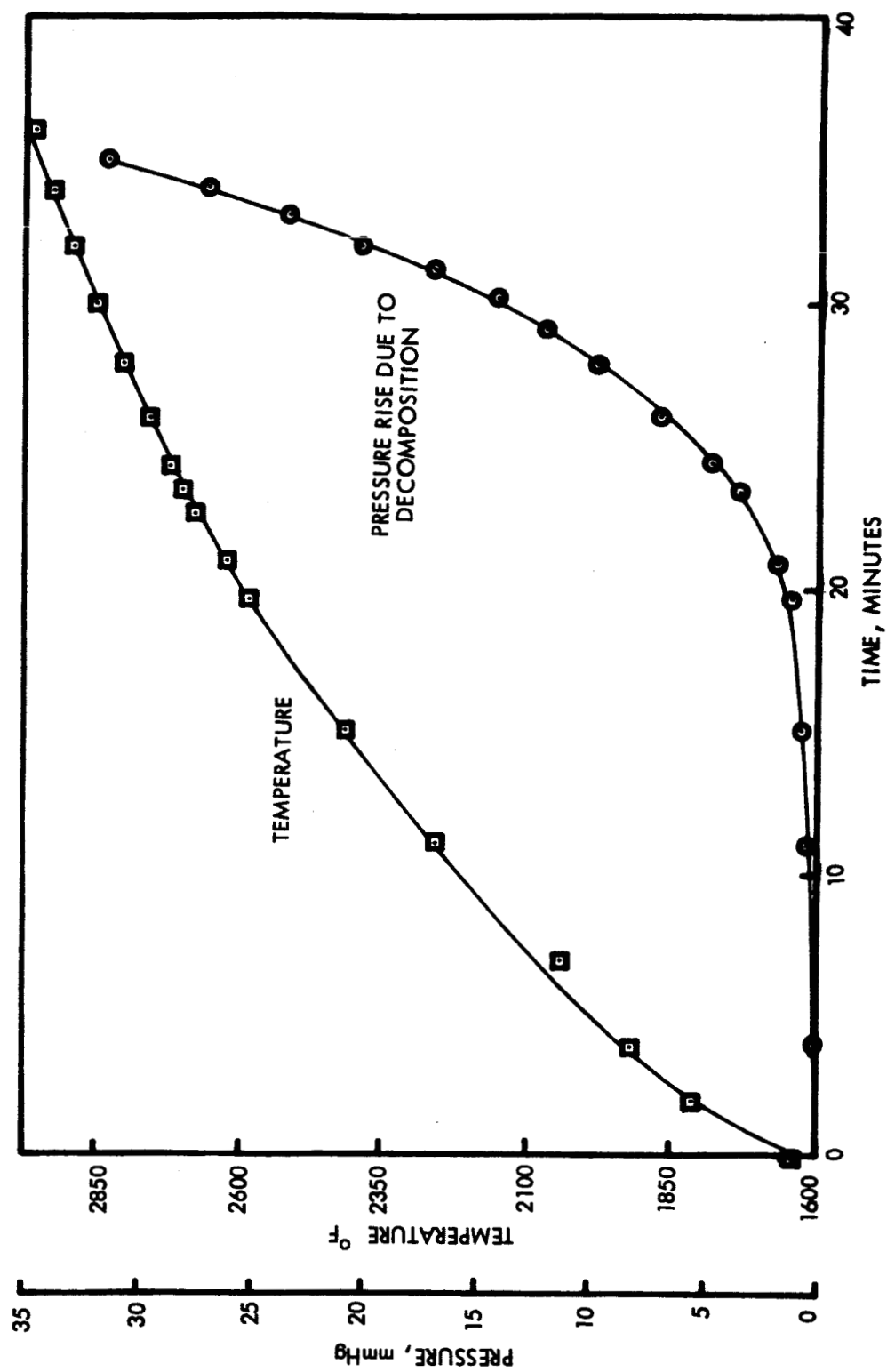


Figure 6.1 High Temperature Reaction Kinetics System



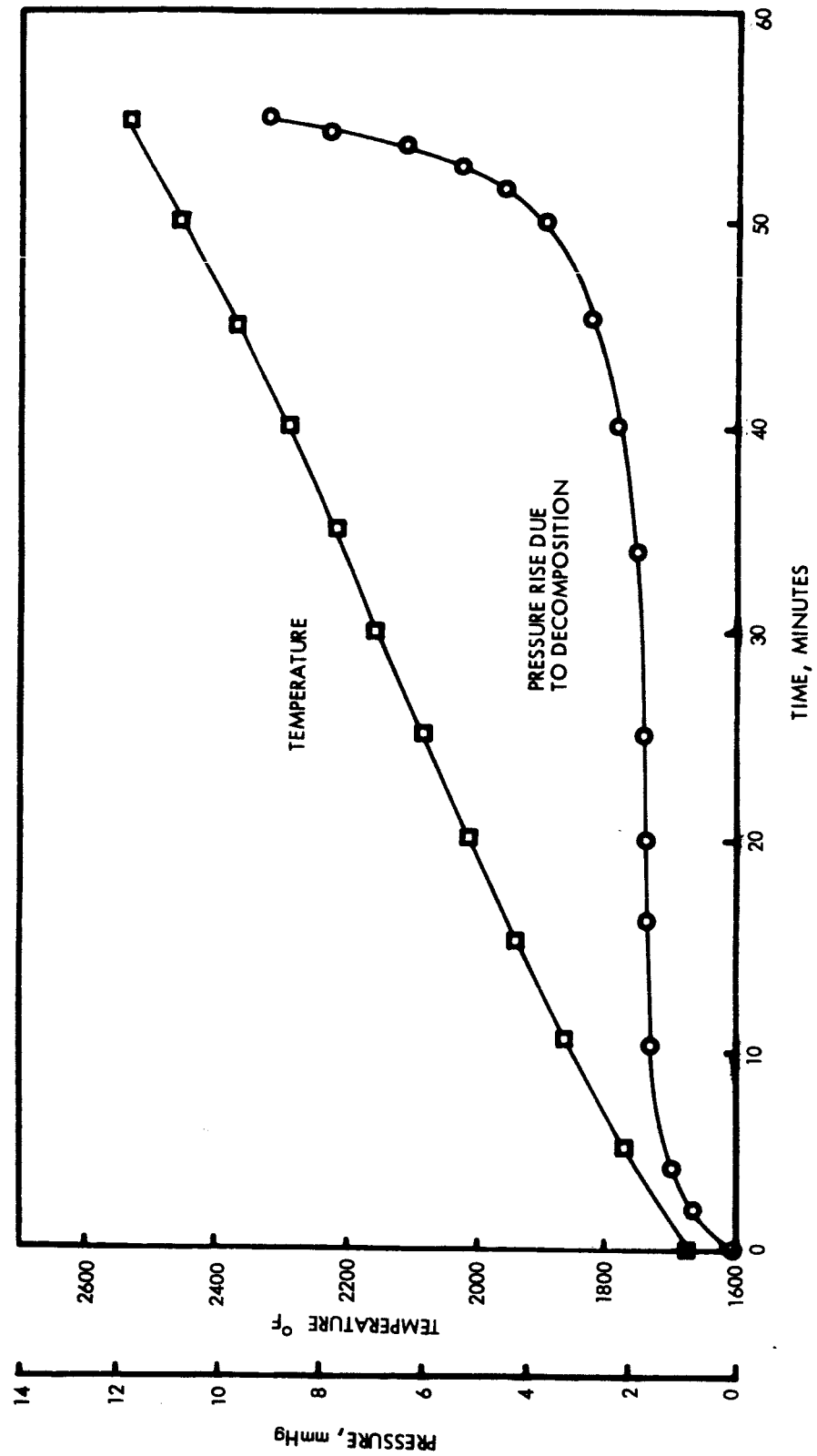


Figure 6.3 Thermal Decomposition of MX 2646 Char

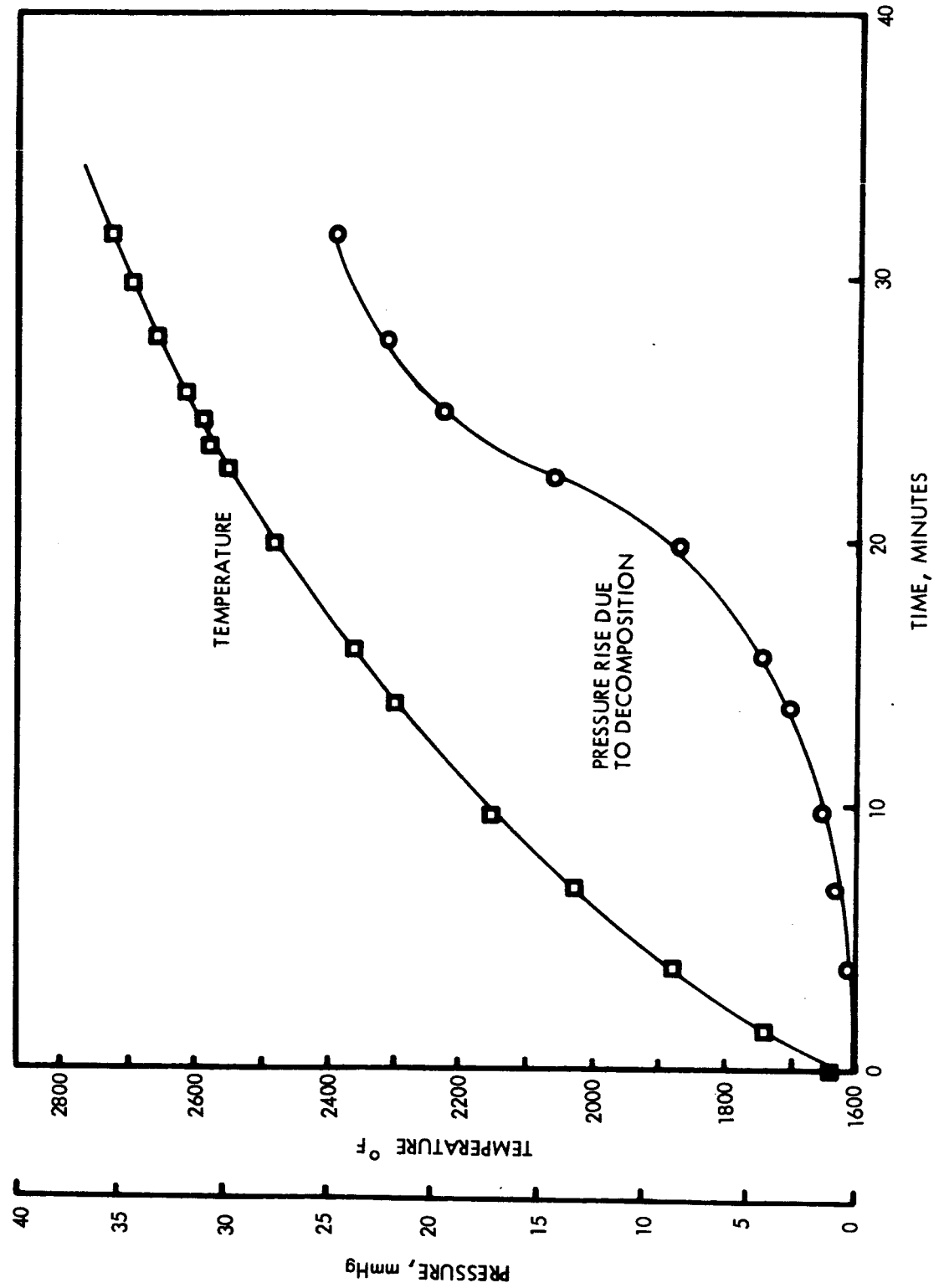


Figure 6.4 Thermal Decomposition of XR 2015 Char

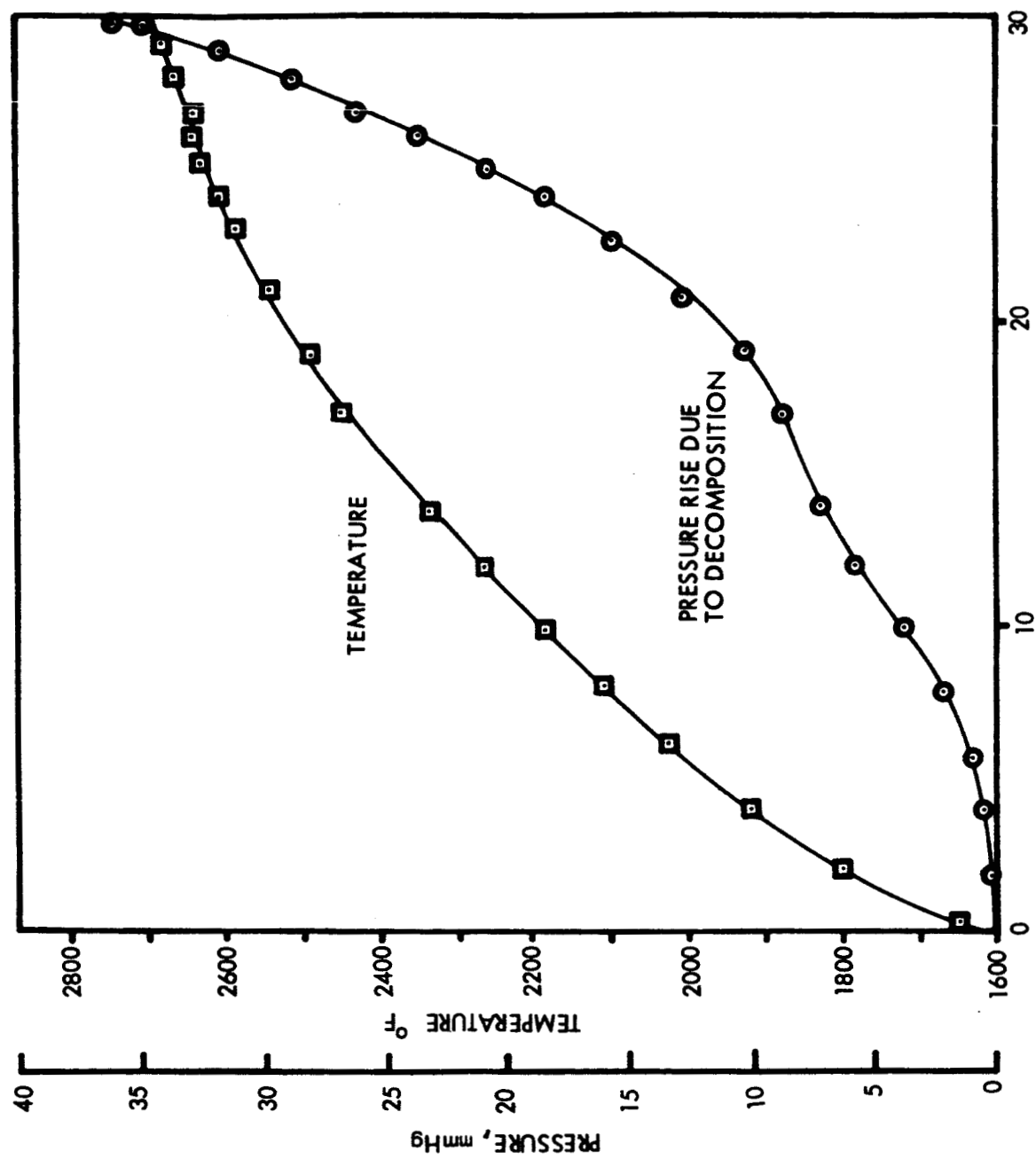


Figure 6.5 Thermal Decomposition of WBC 2234 Char